MICROBIOLOGY SOCIETY

The virulome of *Streptomyces scabiei* in response to cello-oligosaccharides elicitors

1.1 Author names

Benoit Deflandre[1, §], Nudzejma Stulanovic[1, §], Sören Planckaert[2], Sinaeda Anderssen[1], Beatrice Bonometti[1], Latifa Karim[3], Wouter Coppieters[3], Bart Devreese[2], and Sébastien Rigali[1,*]

1.2 Affiliation

[1]InBioS-Centre for Protein Engineering, Institut de Chimie B6a, University of Liège, B-4000, Liège, Belgium.

[2]Laboratory for Microbiology, Department of Biochemistry and Microbiology, Ghent University, B-9000, Ghent, Belgium

[3]Genomics Platform, GIGA, University of Liège, B-4000, Liège, Belgium

[§]B.D. and N.S. contributed equally to this work

1.3 Corresponding author

*Corresponding author: srigali@uliege.be

1.4 Keyword

Common scab disease; Plant host interaction; Plant colonization; plant pathogen; Metabolomics; Biosynthetic Gene Cluster.

1.5 Repositories:

RNAseq data were publicly deposited, and our experimental and analytical pipeline were described on the GEO database repository (Accession number: GSE181490)

2. Abstract

The development of spots or lesions symptomatic of the common scab disease on root and tuber crops is caused by few pathogenic *Streptomyces* with *Streptomyces scabiei* 87-22 as the model species. Thaxtomin phytotoxins are the primary virulence determinants, mainly acting by impairing cellulose synthesis, and their production in *S. scabiei* is in turn boosted by the cello-oligosaccharides released from host plants. In this work we aimed to determine which molecules and which biosynthetic gene clusters (BGCs) of the specialized metabolism of *S. scabiei* 87-22 show a production and/or transcriptional response to cello-oligosaccharides. Comparative metabolomic and transcriptomic analyses revealed that molecules of the virulome of *S. scabiei* induced by cellobiose and cellotriose include i) thaxtomins and concanamycins phytotoxins (and to a lesser extent N-coronafacoyl-L-isoleucine), ii) desferrioxamines, scabichelin and turgichelin siderophores in order to acquire iron essential for housekeeping functions, iii) ectoine for protection against osmotic shock once inside the host, and iv) bottromycins and concanamycins antimicrobials possibly to prevent other microorganisms from colonizing the same niche. Importantly, both cell-oligosaccharides reduced the production of the spore germination inhibitors germicidins and the plant growth regulators rotihibins. The metabolomic study also revealed that cellotriose is in general a more potent elicitor of the virulome compared to cellobiose. This result supports an earlier hypothesis that suggested that the trisaccharide would be the real virulence-triggering factor released from the plant cell wall through the action of thaxtomins. Interestingly, except for thaxtomins, none of these BGCs' expression seems to be under direct control of the cellulose utilization repressor CebR suggesting the existence of another master regulator sensing the internalization of cello-oligosaccharides. Finally, we found nine additional cryptic and orphan BGCs that have their expression awakened by cello-oligosaccharides, demonstrating that other and yet to be discovered metabolites are part of the virulome of *S. scabiei*.

3. Impact statement

Unveiling the environmental triggers that signal proper conditions for host colonization and what is the composition of the arsenal of metabolites specialized for this task (the virulome) is key to understand host-pathogen interactions. In this work, focused on the induction of the common scab disease caused by *Streptomyces* species, we provided further knowledge to both aspects i.e., i) highlighting the capability of cellotriose to trigger the entire virulome and not only the production of thaxtomin phytotoxins, and ii) identifying the set of metabolites that specifically respond to cello-oligosaccharides emanating from the plant under attack. Importantly, we also revealed that the expression of nine cryptic/orphan biosynthetic gene clusters (BGCs) involved in the production of unknown compounds was drastically activated upon cello-oligosaccharides import suggesting that a significant part of the virulome of *S. scabiei* remains to be discovered. Finally, we unexpectedly found that the expression control of most of the known and cryptic BGCs does not depend on the cello-oligosaccharide utilization repressor CebR which suggests the existence of another and yet unknown master regulator of the virulence in *S. scabiei*.

4. Significance as a BioResource to the community

Not Applicable

5. Outcome

Not Applicable

6. Data summary

[A section describing all supporting external data including the DOI(s) and/or accession numbers(s), and the associated URL.]

The authors confirm all supporting data, code and protocols have been provided within the article or through supplementary data files. RNAseq data were publicly deposited, and our experimental and analytical pipeline were described on the GEO database repository (Accession number: GSE181490)

7. Introduction

Streptomyces scabiei (syn. *S. scabies*) is responsible for causing the disease called "common scab" (CS) on root and tuber crops. Together with a dozen of other phylogenetically related *Streptomyces* species, *S. scabiei* colonizes and infects underground storage organs like potato tubers, beets, radishes, turnips, carrots, and peanuts (1,2). CS lesions cause significant economic losses throughout the world, with potato being the most affected crop. The range of symptoms and lesion morphologies on potato tubers goes from superficial to raised or deep-pitted scabs (3). Although CS is characterized by skin defects, it mostly affects the visual aspect of the tuber tissues and root, sometimes also reducing their size, causing a significant drop in the quality and marketability of the potato tubers (3).

The virulence factors which predominantly contribute to the development of CS are the thaxtomin phytotoxins which are nitrated diketopiperazines (4). Eleven thaxtomin analogues have been identified up to date, thaxtomin A being the predominant form associated with the disease (5–7). While the molecular targets are still unknown, thaxtomin A alters the expression of host genes involved in cellulose biosynthesis, cell wall remodeling and strengthening (8,9). Cellulose synthase complexes were also shown to be affected in their density and motility (8), possibly due to endocytosis triggered by thaxtomin A (10). *In vivo*, thaxtomin A causes multiple symptoms to plant targets (11)including necrosis, perturbation of ion fluxes, cell hypertrophy, callose deposition, and ectopic lignin formation. In addition, wounded or immature sites are affected, inducing synthesis of hemicellulose and pectins and leading to the deposition and excessive accumulation of layers of periderm (12).

Next to thaxtomins, other specialized metabolites are known or predicted to play important roles in plant colonization and infection by *S. scabiei*. Several studies revealed that concanamycins and coronafacoyl phytotoxins also contribute to the development of plant disease (11). In synergy with thaxtomins, concanamycins were shown to play an essential role in the type and morphology of developed lesions (13). Contrary to concanamycins and thaxtomins, the exact roles of coronafacoyl phytotoxins in CS disease development are still relatively vague and were shown to be non-essential for pathogenicity development (11). However, their impact via modulating jasmonate hormone signalling networks could assist in overcoming host defence mechanisms (14). N-coronafacoyl-l-isoleucine (CFA-Ile) is the major product of the coronafacoyl gene cluster (15). A wide spectrum of virulence-associated activities of CFA-Ile, like tissue hypertrophy, leaf chlorosis and inhibition of root elongation, were reported in plants. Nevertheless, coronafacoyl phytotoxins are found in non-pathogenic *Streptomyces* spp. as well, suggesting some additional unidentified roles along with the already cited disease-related activities (16). Recently, the production of two novel phytotoxic metabolites was highlighted in *S. scabiei*. Rotihibins C and D are lipopeptides that significantly reduce the photochemistry efficiency of the photosystem II which in turn affects the growth of *Arabidopsis thaliana* and *Lemna minor* at low concentrations. At even lower concentrations, *L. minor* plantlets exhibit an increase in their surface area, suggesting a hormetic effect of rotihibins (17).

Siderophores are also key metabolites for host infecting bacteria, iron being indispensable for housekeeping functions such as DNA replication and protein synthesis. Next to desferrioxamines that are essential for *Streptomyces* survival in iron limited environments (18), *S. scabiei* and related species have the ability to produce diverse and specific

siderophores including scabichelin and turgichelin (19), as well as pyochelin (20) together with three other yet unknown iron chelators deduced from genome mining analysis. This multitude of siderophores with high affinity for ferric iron would guarantee *S. scabiei* to capture iron trapped in its hosts. However, although iron acquisition might contribute to the onset of pathogenicity, *in planta* bioassays showed that there is no connection between virulence and pyochelin production by *S. scabiei* (20).

How *S. scabiei* senses the presence of its plant host and triggers its specialized metabolism required for virulence has also been a main research topic. Induction of thaxtomin biosynthesis requires the import of cello-oligosaccharides (cellobiose and/or cellotriose) by the sugar ABC transporter composed by CebE as the sugar-binding component, CebF and CebG as components of the membrane permease, and MsiK to provide energy to the transport via ATP hydrolysis (21–23). Once inside the cytoplasm, the imported cello-oligosaccharides inhibit the DNA-binding ability of the transcriptional repressor CebR which in turn allows the expression of the *txt* cluster pathway-specific activator TxtR (22,24).

If the path from cello-oligosaccharide uptake to activation of thaxtomin biosynthesis is well described at the molecular level, many questions remain unsolved. The first issue regards cellobiose itself as a natural environmental elicitor of the CS disease. Most *in vivo* and *in vitro* studies on the induction of the pathogenic lifestyle of *S. scabiei* used cellobiose and not cellotriose as the triggering factor. The only reason why cellotriose is usually excluded from laboratory studies is because it is much more expensive and less available in large quantities compared to cellobiose. However, earlier studies suggested that cellobiose is unlikely to be

144 released from plant cell wall depolymerization by thaxtomins during host colonization by *S.*
145 *scabiei*. Instead, incubation of tobacco and radish seeds with thaxtomin A showed release of
146 cellotriose (25). Cellobiose on the other hand, is an important by-product of cellulose
147 hydrolysis by the cellulolytic system, which naturally occurs upon organic matter turnover by
148 the soil microflora. However, the ability of *S. scabiei* to degrade cellulose is insignificant
149 despite possessing a complete cellulolytic system (25–27). While the molecular mechanism
150 silencing the cellulolytic system of *S. scabiei* is unknown, it avoids the release of cellobiose
151 from decaying plant biomass, hence preventing this bacterium to be a protagonist in the
152 mineralization of organic soils. This particularity could be a major evolving adaptation that
153 somehow "forces" *S. scabiei* to instead colonize living plant tissues. Sensing cellotriose
154 released by the depolymerization of cellulose caused by thaxtomin, together with silencing
155 the cellulolytic system and thus avoiding the release of cellobiose, could allow this bacterium
156 to discriminate if cellulose by-products originate from living or instead dead plant cell walls
157 (25,27).

158 An even more important question that remains to be solved is the exact composition of the
159 arsenal of specialized metabolites that constitute the virulome of *S. scabiei*. Are thaxtomins
160 the only phytotoxins that respond to virulence elicitors or do other specialized metabolites
161 display the same production response? Recently, the group of Prof Dawn Bignell has shown
162 that cultivation of *S. scabiei* in the oat bran agar (OBA) medium is not only able to induce
163 thaxtomin production, but also other specialized metabolites known or predicted to play an
164 important role in colonizing and infecting the plant host tissues, i.e., CFA-Ile,
165 concanamycins, siderophores (desferrioxamines and pyochelin), and also a form of auxin
166 (IAA) (28). OBA is a complex plant-based medium in which cello-oligosaccharides are

167 proposed to be responsible for the induction of thaxtomin production (25). However, it
168 cannot be excluded that some of the other compounds present in OBA influence – positively
169 or negatively, alone or in combination – the production of specialized metabolites.

170 As previous studies suggested cellobiose and/or cellotriose to be natural elicitors of the
171 pathogenic response of *S. scabiei* (27), their specific contribution to the induction of the
172 metabolome requires further investigation. In this work we wanted to provide answers to
173 whether cellotriose could – equally to cellobiose – trigger the "virulome" of *S. scabiei* and if
174 the cello-oligosaccharide mediated induction takes place at the transcriptional level. Our
175 work revealed that cellotriose is a better inducer of the virulome of *S. scabiei* compared to
176 cellobiose. Our transcriptomic analysis also shows that cryptic/orphan biosynthetic gene
177 clusters have their expression awakened by cello-oligosaccharides suggesting that yet
178 unknown metabolites would be part of the virulome of *S. scabiei*.

179

8. Methods

Strain and culture conditions

Streptomyces scabiei 87-22 and its *ΔcebR* mutant (22) were routinely cultured in Tryptic Soy broth (TSB, 30 g/l, Sigma-Aldrich) or ISP2 (for 1l: 4 g Yeast Extract, 10 g Malt Extract, 4 g Dextrose, pH 7.2) liquid media at 28°C under shaking (180 rpm, New Brunswick™ Innova® 44 incubator shaker). Modified thaxtomin defined medium (TDM) ((25), without L-Sorbose) was used as minimal medium, supplemented with maltose 0.5% (Sigma-Aldrich) in which cellobiose (Carbosynth) and cellotriose (Megazyme) were added as inducers. Sucrose (saccharose) was purchased from Merck.

Transcriptomics

Cultures and sampling

Pre-cultures of *S. scabiei* 87-22 (WT) and Δ*cebR* were conducted in 50 ml ISP2 medium inoculated with $4*10^7$ spores for 24 hours. The mycelium was collected by centrifugation (3,500 g for 5 minutes at room temperature (RT)) and washed twice by resuspension/centrifugation with 20 ml TDM medium without carbon source. The mycelium was then resuspended in TDM + maltose 0.5% (TDMm) or ISP2 to a density of 16 mg/ml (wet biomass) and then split into three Erlenmeyer flasks (per strain and culture condition) containing a culture volume of 25 ml. After 30 minutes of incubation in TDMm at 28 °C, a first sampling (= time points 0) of 2.5 ml was collected from each flask and cellobiose or cellotriose were added to a final concentration of 2.5 mM, each into three flasks. The next samplings were collected following the same procedure, 1 and 2 hours (= time points 1 and 2,

respectively) post addition of cello-oligosaccharides. In the ISP2 culture condition involving *S. scabiei* WT and Δ*cebR*, 2.5-ml samples were collected in each flask after 3 hours of culture. All samples were collected in 15-ml Falcon tubes and centrifuged for 3 minutes at 3,500 g (RT). The supernatant was quickly and thoroughly removed, and the tubes were immediately flash-frozen into liquid nitrogen. The frozen cell pellets were placed into a -80 °C freezer until RNA extraction.

RNA preparation

The RiboPure™ Bacteria RNA Purification Kit (Invitrogen) was used for total RNA extraction. The RNAwiz lysis buffer was added to the frozen mycelium pellets and the procedure was followed according to the manufacturer's guidelines except the bead-beating step that was extended to 20 minutes. The quantification and quality control of total RNA samples were performed on a Bioanalyzer 2100 (Agilent). Ribosomal RNA depletion and library preparation were carried out using the Ovation Complete Prokariotic RNAseq kit (NuGEN). The libraries were sequenced on a NextSeq® 500 System (Illumina) HM 2X75 bp read length with 7 million reads per library.

Read mapping and differential expression

Sequenced reads were quality-checked and trimmed when necessary, using the Trimmomatic Software (29). Reads were subsequently mapped to the reference genome (*S. scabiei 87-22*), using Bowtie2 (30,31), and an average of 98.7% of reads were aligned. For each transcript, the number of mapped reads were compiled with featureCounts (32), outputting a count table on which the rest of the analysis is based. Differential expression analysis was performed in

222 R, with the DESeq2 package (33). RNAseq data were publicly deposited, and our
223 experimental and analytical pipeline were described on the GEO database repository
224 (Accession number: GSE181490)

225 **Metabolomics**

226 After 45 hours of pre-culture in TSB inoculated with $2*10^7$ spores of *S. scabiei* 87-22, the
227 mycelium was collected by centrifugation (3,500 g for 5 minutes at RT) and washed twice by
228 resuspension/centrifugation with 20 ml TDM medium without carbon source. The washed
229 mycelium was resuspended to a density of 200 mg/ml (wet biomass) and 1 ml was used to
230 inoculate TDM + maltose 0.5 % (TDMm) plates (25 ml) as overlay. Four conditions were
231 tested with three biological replicates: TDMm; TDMm + cellobiose 2.5 mM; TDMm +
232 cellotriose 2.5 mM; TDMm + sucrose 2.5 mM. After 96 hours of incubation at 28 °C, one
233 half of each plate was extracted with mQ H_2O (v/v), dried, resuspended in 1 ml of mQ H_2O,
234 and filtered through 0.22 µm syringe-driven filters. These metabolic extracts were diluted 20
235 times in 97/3/0.1 H_2O/ACN/HCOOH to improve chromatographic and mass spectrometric
236 performance.

237 The µLC-MS/MS system consisted of a Waters NanoAcquity M-Class UPLC coupled to a
238 Waters Xevo TQ-S triple quadrupole mass spectrometer fitted with an IonKey/MS^{TM} source
239 (Waters, MA, USA). Mobile phase A was 0.1% formic acid in H_2O (Biosolve) and mobile
240 phase B was 0.1% formic acid in acetonitrile (Biosolve). The strong and weak solutions used
241 to wash the auto-sampler were 0.1% HCOOH in H_2O and 0.1% HCOOH in
242 acetonitrile/water/isopropanol (Biosolve) (50:25:25, v/v/v), respectively. The samples were
243 directly injected (5 µl injection volume) to a Waters 150 µm x 100 mm, 1.8 µm HSS T3,

iKey^{TM} separation device. The metabolites were eluted from the analytical column using the following gradient: 0-10 min: 3-50% B, 10-11 min: 50-80% B, 11-15 min: 80% B, 15-16 min 80-3% B, 16-25 min: 3% B at a flow rate of 2 µl/min. The column was operated at 45°C, ionization was performed in positive mode using a voltage of 3.65 kV. The cone and collision voltage were set respectively at 35 V and 30 V, and the source temperature was 120°C.

Detection was obtained by MRM mode with transitions of the analytes of interest and their specific retention window (± 0.5 min). Selection of these transitions was based on information in the GNPS public spectral library, literature survey, optimization experiments and own findings (17) (Table S1). Data acquisition was performed by MassLynx 4.2 software, and the data was subjected to a Savitzky-Golay smoothing in Skyline v21 (Adams et al. 2020). The Area Under the Curve (AUC) of ion peaks was calculated and normalized to the TDMm condition for each metabolite. Each complete set of different conditions/biological replicates were randomly analysed and separately repeated (triplicates).

Genome mining

AntiSMASH (antibiotics and secondary metabolites analysis shell; version 5.1.2), available at https://antismash.secondarymetabolites.org, was used for genome mining (34) in combination with the internal MIBiG 2.0 (Minimum Information about a Biosynthetic Gene cluster) database (35). The complete genome sequence of *Streptomyces scabiei* 87-22 (Ref NC_013929) was used for the prediction of BGCs. Manual inspection was carried out to rectify the synteny values provided by AntiSMASH, only considering protein sequences sharing a minimum of 60% of identity on at least 70% of sequence coverage. BGC

265 delimitation and/or attribution issues were manually corrected and supported by literature
266 survey.

267

9. Results

The specialized metabolism of *S. scabiei* 87-22

Prior to assessing the transcriptomic and metabolomic responses of *S. scabiei* 87-22 to virulence elicitors, we updated the current knowledge on the BGCs of the specialized metabolism of this species. A genome mining analysis has recently been performed by Liu et al. (28), identifying 34 BGCs including eight terpenes, six non-ribosomal peptide synthetases (NRPSs), six polyketide synthases (PKSs), one hybrid PKS-NRPS BGC, five ribosomally synthesized and post-translationally modified peptides (RiPPs), four siderophores, and four other types of BGC (betalactone, butyrolactone, melanin, and ectoine). We performed additional and manual rounds of inspection (additional BLAST searches and a literature survey) in order to i) identify possible BGC delimitation issues and correct BGC length, ii) split individual BGCs into multiple BGCs, and iii) identify BGCs involved in the production of known natural products absent from the MIBiG database (version 2.0). In total, 12 other BGCs were identified through these additional steps leading to a final list of 46 BGCs (Table 1). Among these 12 additional BGCs, there was only one BGC for which the natural product is known, namely BGC#33b coding for melanin. The other 11 BGCs, including BGC#1b (NRPS), BGC#6b (terpene), BGC#7b (bacteriocin), BGC#16b (lanthipeptide), BGC#23b (butyrolactone), BGC#23c (LAP), BGC#23d (PKS), BGC#27a (Type 1 PKS), BGC#29a (Type 3 PKS) and BGC#31b (linaridin) display relatively low similarity levels with genes of BGCs associated with the biosynthesis of known compounds (Table 1).

Over a third of the predicted BGCs (18 out of 46) encode genes involved in the production of natural products that have already been identified in *S. scabiei* or in other *Streptomyces*

290 species (known BGCs) (Table 1). Half of these (9 out of 18) belong to the so-called core
291 metabolome (36) i.e., BGCs involved in the biosynthesis of molecules produced by almost all
292 *Streptomyces* species including 2-methylisoborneol (BGC#5), isorenieratene (BGC#6a),
293 hopene (BGC#9), geosmin (BGC#12), the WhiE spore pigment (BGC#17), desferrioxamines
294 (BGC#21), melanins (BGC#22, BGC#33b), and ectoine (BGC#24). The remaining 9 BGCs
295 of known metabolites were classified into three different functional categories, namely, i)
296 plant-associated molecules (thaxtomins, the coronafacoyl phytotoxins, concanamycins, and
297 rotihibins), ii) siderophores (pyochelin, scabichelin and turgichelin, in addition to
298 desferrioxamines), and iii) antimicrobials (informatipeptin, bottromycins, and germicidins).
299 Note that concanamycins also exhibit antiviral (37) and antifungal (38) activities due to their
300 capacity to inhibit the V-type H^+ ATPase (39) and therefore could also have been included
301 into the "antimicrobials" functional category.

302 The remaining 28 BGCs are considered as "cryptic" or "orphan", i.e., either their product is a
303 yet undiscovered natural product (unknown unknowns) or is a known compound but the
304 genetic material responsible for its synthesis is still unknown (unknown knowns) (40).
305 Nevertheless, different types of natural products deduced by antiSMASH allowed us to sort
306 these BGCs into different categories. Genome mining predicted four NRPSs (BGC#1b, #11a,
307 #11b, #25), four terpenes (BGC#6b, #14, #26, #30), four PKSs (BGC#23a, #23d, #27a,
308 #29a), three siderophores (BGC#10, #15, #32), three lanthipeptides (BGC#4, #16b, #19), two
309 bacteriocins (BGC#7b, #13), two butyrolactones (BGC#8, #23b), one LAP (BGC#23c), one
310 indole (BGC#27b), one linaridin (BGC#31b), one betalactone (BGC#2), and one hybrid
311 PKS-NRPS BGC (BGC#18) (Table 1).

312 **Specialized metabolite production upon sensing cellobiose and cellotriose**

313 The effect of cello-oligosaccharides cellobiose and cellotriose on the induction of the
314 specialized metabolism of *S. scabiei* 87-22 was assessed by targeted liquid chromatography-
315 multiple reaction monitoring MS (LC-MRM-MS). Figure 1 shows the Area Under the Curve
316 (AUC) of ion peaks related to known metabolites produced by *S. scabiei* 87-22 (Table S1)
317 when cultured with or without the environmental virulence elicitors cellobiose and
318 cellotriose. Expectedly, thaxtomin A was about 5- and 7-fold overproduced in TDMm +
319 cellobiose and in TDMm + cellotriose, respectively. The greatest production of thaxtomin A
320 appeared to occur upon culture in the presence of cellotriose compared to cellobiose,
321 confirming earlier results suggesting that the trisaccharide has a higher triggering effect on
322 thaxtomin phytotoxin biosynthesis (25). Concanamycins A and B followed the same
323 production pattern with stronger induction rates: on average 16- and 30-fold increases in
324 metabolite levels were observed in TDMm + cellobiose and in TDMm + cellotriose,
325 respectively (Figure 1). In contrast, N-coronafacoyl-L-isoleucine (CFA-Ile) was not
326 strikingly overproduced compared to other plant-associated metabolites. Indeed, we only
327 observed about 2-fold overproduction in both conditions where cello-oligosaccharides were
328 added, and the condition including sucrose displayed similar CFA-Ile levels (Figure 1).

329 Regarding the production patterns of the siderophores produced by *S. scabiei* 87-22, both
330 desferrioxamines (B and E) showed enhanced production when *S. scabiei* 87-22 was grown
331 in the presence of cellobiose or cellotriose, with a pattern similar to that observed for
332 thaxtomin A and concanamycins. Desferrioxamine E was the most overproduced of the two,
333 especially in TDMm + cellotriose with an average of 19-fold increase in its abundance levels

(Figure 1). Scabichelin and turgichelin – both synthesized by BGC#33a – followed the same trend as desferrioxamines: production increases of about 15- and 25-fold were observed upon addition of cellobiose and cellotriose, respectively. By contrast, pyochelin production was not influenced by either of the cello-oligosaccharides, while sucrose had a limited positive effect of about 2-fold on the siderophore abundance (Figure 1).

The production of bottromycins A2 and B2, as well as its other detected forms (D and E, data not shown), positively responded to the addition of cellobiose and cellotriose (Figure 1). While there was on average a 13-fold overproduction of these antimicrobial metabolites following the addition of cellobiose, cellotriose triggered about twice as much (28-fold increase) production of bottromycins. The production of the osmoprotectant ectoine also positively responded to the presence of cellobiose and cellotriose, with 14- and 26-fold overproduction, respectively (Figure 1).

Out of all the analysed metabolites, only two types of compounds had their relative abundance decreased upon cello-oligosaccharide supply i.e., germicidins and rotihibins. Germicidin A, the inhibitor of *Streptomyces* spore germination, showed a significant decrease in its production levels in both conditions containing cello-oligosaccharides – about 3-fold in TDMm + cellobiose and 10-fold in TDMm + cellotriose (Figure 1). The production of germicidin B displayed the same pattern (data not shown). Similarly, both rotihibins (C and D), recently identified as a novel category of herbicides produced by *S. scabiei* (17), were strongly underproduced with decreases of about 30-fold following cellobiose and cellotriose supply. The addition of sucrose also reduced the amount of rotihibins detected, but to a lower extent (about 5-fold reduction) (Figure 1).

356 **Tanscriptional response of BGCs to cellobiose and cellotriose**

357 **BGC of known metabolites under expression control of cello-oligosaccharides**

358 Next to the metabolomic study described above, we also assessed which BGCs responded to
359 the environmental triggers cellobiose and cellotriose at the transcriptional level by RNA-seq.
360 For this, RNA samples were collected 1 and 2 hours post addition of cellobiose and
361 cellotriose (see Methods for details). From all expression data, we focused on the genes
362 belonging to the 18 BGCs involved in the production of known specialized metabolites of *S.*
363 *scabiei* 87-22 (Table 2, Figure 2). We only considered the expression data of the core
364 biosynthetic gene(s) of each BGC (Table S2) in order to have the best possible correlation
365 between the transcriptomic data and the metabolomic study described earlier. The
366 transcriptional response of the core biosynthetic genes of these "known" BGCs upon supply
367 of cellobiose and cellotriose is displayed in Figures 2A and 2B, respectively, and fold-change
368 values for the core biosynthetic genes of each BGC are displayed in Table 2.

369 The thaxtomin biosynthesis cluster, designated here as BGC#16a (Table 1), contains two
370 genes whose expression is known to be triggered by both cellobiose and cellotriose (25).
371 Therefore, the response of these core biosynthetic genes, *txtA* (*scab_31791*) and *txtB*
372 (*scab_31781*), can be regarded as "positive controls" for cellobiose/cellotriose upregulated
373 genes. As anticipated, both carbohydrates could drastically increase the transcription of
374 thaxtomin biosynthetic genes. The best transcriptional activation response for *txtA* and *txtB*
375 was observed in the cellobiose condition, i.e., 28- and 56-fold upregulation 2 hours post
376 induction for *txtA* and *txtB*, respectively (Table 2, Figure 2A). Cellotriose was similarly able
377 to activate the expression of both genes, with the biggest fold change also observed at 2 hours

post induction, i.e., 10- and 17-fold upregulation for *txtA* and *txtB*, respectively. Analysis of the expression patterns of the other *txt* genes revealed that the whole BGC positively responds to both elicitors, *txtC* displaying the best transcriptional response in the cellobiose condition, with a 143-fold increased expression at 2 hours post induction (Supplementary Figure S1). Overall, the results obtained for the *txt* cluster demonstrate that our experimental set up is appropriate to assess the transcriptional response when *S. scabiei* 87-22 triggers the expression of its main virulence determinant.

Regarding the other BGCs involved in the production of plant-associated molecules, results from the metabolomic and transcriptomic approaches corroborate. As mentioned above, the production of concanamycins was highly responsive to both cello-oligosaccharides. The transcriptomic study confirms this, as the expression of the core biosynthetic genes of BGC#31a, namely *conABCDEF*, showed an average of 2.6- and 3-fold upregulation in cellobiose and in cellotriose, respectively. Genes of BGC#28 responsible for CFA-Ile production also showed a very strong positive expression response to both cello-oligosaccharides (an average of 14- and 19-fold upregulation for cellobiose and cellotriose, respectively), which is in line with the two-fold overproduction of CFA-Ile induced by both cello-oligosaccharides (Table 2, Figure 2). Finally, the analysis of the biosynthetic genes of rotihibins (BGC#3) revealed that the expression of core genes of this cluster does not specifically responds to either cellobiose or cellotriose (Table 2, Figure 2), while the results of our metabolomic analysis suggested a possible down-regulation (Figure 1).

Regarding the biosynthetic genes of desferrioxamines (BGC#21), scabichelin and turgichelin (BGC#33a) siderophores, their expression was also greatly influenced by both saccharides.

Transcription of genes responsible for desferrioxamines biosynthesis displayed their greatest response 2 hours post induction for both elicitors, i.e., 40- and 27-fold upregulation for cellobiose and cellotriose, respectively. Biosynthetic genes of BGC#33a involved in scabichelin and turgichelin production were similarly positively affected by cellobiose and cellotriose with an average of 13- and 9-fold upregulation, respectively (Table 2, Figure 2). However, the expression of pyochelin biosynthetic genes (BGC#1a) remained quite steady upon addition of either cello-oligosaccharides, which tends to confirm the metabolomic data (Table 2, Figure 2).

Regarding the BGCs responsible for the production of the antimicrobial compounds bottromycins, and informatipeptin, none of them showed transcriptional activation upon addition of either cellobiose or cellotriose (Table 2). Indeed, the transcription of BGC#20 (for bottromycins) displayed contradicting transcriptional responses (up-regulated or no change at 1 h post induction and down-regulated at 2 h post induction, Figure 2), that overall are not in line with the remarkable overproduction observed via the comparative metabolomic approach (Figure 1, see Discussion). BGC#7a, which shows about 60% synteny to the antimicrobial lanthipeptide informatipeptin, has an expression pattern that was neither influenced by cellobiose nor cellotriose (Table 2, Figure 2). Finally, BGC#29b associated with germicidin production is one of the rare BGCs for which transcriptomic and metabolomic analyses do not correlate, as the absence of transcriptional response is not in line with the marked decrease in production presented in Figure 1 (see Discussion).

Regarding the nine BGCs which belong to the so-called core metabolome of *Streptomyces* species, the addition of cello-oligosaccharides only significantly influenced the expression of

422 BGC#5 (2-methylisoborneol), BGC#12 (geosmin), and BGC#22 (melanin) (Figure 2, Table
423 2). The effect of both inducers on the expression of the desferrioxamine BGC – which is part
424 of the core metabolome – has already been discussed in the section associated with
425 siderophore BGCs. Cellobiose and cellotriose both activated expression of BGC#5 at almost
426 the same level – around 3-fold, whereas only cellotriose had an impact on the expression of
427 the biosynthetic genes of BGC#22 with an average of 7-fold upregulation. Regarding the
428 osmoprotectant ectoine (BGC#24 in Table 1), we did not observe any significant expression
429 change which does not correlate with the overproduction measured via the metabolomic
430 approach.

431 **Cryptic BGCs transcriptionally activated by cello-oligosaccharides**

432 Aside from the 18 BGCs involved in the production of known metabolites, we also assessed
433 the effect of each cello-oligosaccharide on the expression level of the 28 cryptic or orphan
434 BGCs deduced from genome mining (Tables 1 and 2). As shown in Figure 3, the expression
435 of nine cryptic BGCs was influenced by cellobiose or cellotriose. Both carbohydrates
436 significantly increased the transcription of five BGCs, namely BGC#1b (NRPS), BGC#7b
437 (bacteriocin), BGC#13 (bacteriocin), BGC#15 (siderophore), and BGC#32 (siderophore)
438 (Table 2). The highest transcriptional response was observed for the genes of BGC#32
439 involved in the synthesis of a siderophore metabolite, which were induced up to 28-fold by
440 cellobiose and 15-fold by cellotriose (Table 2, Figure 3). The transcription of another BGC
441 coding for an unknown siderophore (BGC#15) was also increased to about 3-fold by both
442 carbon sources (Table 2, Figure 3). Interestingly, both bacteriocin types of metabolites, i.e.,
443 BGC#7b and BGC#13, were upregulated by both cello-oligosaccharides. BGC#13 was

equally upregulated by both sugars (around 3-fold), whereas the transcriptional response of BGC#7b was induced more by cellotriose (5.5-fold) compared to cellobiose (2.7-fold). The presence of the cellobiose and cellotriose also positively influenced the transcription of two unknown NRPS BGCs (BGC#1b and BGC#25) with an average 5-fold change for BGC#1b and around 2-fold change for BGC#25 (Table 2, Figure 3).

Four other BGCs had their expression upregulated by only one of the two tested cello-oligosaccharides. Cellobiose could in addition induce the expression of BGC#14 (terpene), BGC#23a (PKS), and BGC#25 (NRPS) (Figure 3A), whereas cellotriose positively impacted the expression of BGC#2 (betalactone) (Figure 3B). Importantly, the expression of the core genes of 19 of the 28 cryptic BGCs remained silent or was not significantly influenced by cellobiose or cellotriose.

Effect of *cebR* deletion on the expression of cello-oligosaccharide-dependent BGCs

The *txt* cluster responsible for thaxtomin production was previously reported to be under direct control of the cellulose utilization repressor CebR (22). Two CebR-binding sites have been discovered within the *txt* cluster which allows the CebR repressor to switch off the expression of the thaxtomin pathway-specific activator TxtR, in turn resulting in the transcriptional repression of the whole thaxtomin BGC. Binding of cellobiose and/or cellotriose to CebR unlocks the system which allows thaxtomin production. According to our transcriptomic analysis, a total of 16 BGCs have their expression increased by the addition of either cellobiose and/or cellotriose (Table 2) suggesting a possible role of CebR as direct transcriptional repressor of other gene clusters of *S. scabiei*. A transcriptome analysis was thus performed in order to assess which BGCs, beyond the *txt* cluster, would also have their

466 expression under control of CebR. For this, *S. scabiei* 87-22 (wild-type) and its *cebR* null
467 mutant (Δ*cebR*) were cultured in ISP2 liquid medium, and RNA samples were collected 3
468 hours after culture inoculation with fresh mycelium. The volcano plot in Figure 4 shows the
469 relative expression of genes that were determined to be "core biosynthetic genes" of the
470 different BGCs (Table S2). As can be seen in this plot (Figure 4), only one "known" BGC
471 shows an increased expression in the Δ*cebR* mutant, which unsurprisingly corresponds to the
472 thaxtomin biosynthetic cluster (BGC#16a). However, three additional cryptic clusters see
473 their core genes' expression increased, namely, BGC#14, #16b, and #32 coding for terpene,
474 lanthipeptide, and siderophore specialized metabolites, respectively. In the case of BGC#16b,
475 we can also observe that only one out of its three core genes fall into the upregulated category
476 ("UP" at Figure 4). Interestingly, BGC#32 also responded positively to cellobiose and
477 cellotriose (Table 2) and BGC#14 also showed upregulation upon cellobiose supply (Table
478 2). However, none of the genes from these cryptic BGCs have been predicted to contain a
479 CebR-binding site (*cbs*) in their upstream region, meaning it is unlikely that their expression
480 would be directly regulated by CebR (see Discussion).

481 Based again on core gene differential expression, there is a total of 6 downregulated BGCs,
482 among which 2 known clusters (BGC#1a and #28), corresponding to the pyochelin and CFA-
483 Ile biosynthetic clusters. However, these 2 known BGCs showed upregulation upon
484 cellobiose and/or cellotriose supply (Table 2) suggesting there is an absence of correlation
485 between the response to cello-oligosaccharides and the inactivation of the DNA-binding
486 ability of CebR. The four cryptic BGCs that are downregulated correspond to types NRPS
487 (BGC#1b), bacteriocin (BGC#13), siderophore (BGC#15), and lanthipeptide (BGC#19).

488

10. Discussion

Conclusions on metabolites that respond to cello-oligosaccharides

Of all the different ways to determine what makes an organism excel in a lifestyle or in an environmental niche, generating mutants and assessing their phenotypic repercussions is the most straightforward approach. However, this approach can sometimes lead to erroneous or questionable conclusions for various reasons, such as gene-function redundancy or genetic compensation mechanisms that could lead to phenotypes that understate the importance of a gene. In studies on the CS disease, finding what is really essential for the virulence of *S. scabiei* and related species is thus obviously subjected to these constraints linked to the use of reverse genetics. For instance, the inactivation of *scab_1471* in *S. scabiei* resulted in a mutant strain unable to produce pyochelin but showing no sign of reduced virulence, indicating that this siderophore is either not essential for pathogenicity, or that its absence is rescued by other siderophore(s) produced by *S. scabiei* (20). Also, the interference with thaxtomin production caused by the inactivation of the cellobiose and cellotriose beta-glucosidase BglC (41) revealed a genetic compensation phenomenon that awakened the expression of alternative beta-glucosidases allowing *S. scabiei* to maintain the capacity to use cello-oligosaccharides (42). The experimental set-ups can also sometimes be suboptimal – such as inappropriate host and/or culture conditions – to observe the real impact of a mutation and therefore to conclude on the role of a gene product in a biological process. This is for example the case of CFA-Ile as gene inactivation in *S. scabiei* showed reduced tissue hypertrophy on potato tuber slices, but the impact of the mutant has only been assessed on tobacco *in vivo* and not on its natural hosts which questions the relevance of this molecule in the colonization process (43). Apart from the results on the mutants involved in the

biosynthesis of thaxtomins (5,22,23,41), it is thus sometimes difficult to draw conclusions on the importance of a BGC in contributing to the capacity of *S. scabiei* to colonize and infect root and tuber plants.

For the above-mentioned reasons, we chose approaches alternative to reverse genetics, i.e., comparative transcriptomic and metabolomic analyses, to determine which part of the specialized metabolism of *S. scabiei* would be dedicated to host infection. Both approaches assume that a large proportion of the molecules/genes required for host colonization will respond to the same elicitors and therefore will display production or expression patterns that are synchronized with the main virulence determinants that, in this case, are the thaxtomin phytotoxins. The results of the metabolomic approach provided a clear picture of the specialized metabolites of *S. scabiei* that have their production specifically modulated by cello-oligosaccharides. The cello-oligosaccharide-dependent known metabolites of the virulome of *S. scabiei* include: i) plant-associated metabolites, namely thaxtomins and concanamycins phytotoxins (and to a lesser extent CFA-Ile), ii) desferrioxamines, scabichelin and turgichelin siderophores, iii) the bottromycin antimicrobials, and iv) the osmoprotectant ectoine. Importantly, of all the known metabolites of *S. scabiei*, germicidins, that are autoregulatory inhibitors of *Streptomyces* spore germination, are metabolites that had their production sensibly reduced. Inhibition of germicidin production following the perception of cellotriose that would emanate from the plant cell wall could be regarded as the first “green light” to allow the onset of the pathogenic lifestyle of *S. scabiei*. Moreover, the production of the plant growth regulators rotihibins was drastically reduced after addition of cellobiose and cellotriose. This response, opposite to the dynamics of thaxtomins, suggests that rotihibins are not part of the virulome of *S. scabiei*. The absence of virulence bioassays on natural host

plants, the presence of clusters homologous to BGC#3 in plant-helping streptomycetes, and the plant growth promoting effect observed at low doses suggest that rotihibins might be involved in another aspect of the plant-associated lifestyle, despite exhibiting phytotoxicity at higher doses (17).

Our work showed that there is also a strong positive biosynthetic response of desferrioxamines, scabichelin and turgichelin siderophores which are molecules usually produced upon sensing low iron concentrations. Siderophores and iron supply are essential for the onset of both metabolite production and sporulation in streptomycetes (44–46). We have also previously shown that when siderophore biosynthesis responds to signals other than the environmental iron concentration, it can have a strong impact on their developmental program (47). Such a synchronized production of phytotoxins and siderophores, though still being a real enigma regarding the molecular mechanism in place, makes perfectly good sense in terms of host colonization. Iron is mandatory for most housekeeping functions while free iron is not available within the hosts. The upregulation of two additional cryptic BGCs predicted to be involved in the biosynthesis of siderophores (see below) further emphasizes the essential role of iron acquisition during host colonization. Interestingly, Liu et al 2021 reported the absence of production of scabichelin and turgichelin in OBA (19,28), suggesting that other compounds present in this more complex medium interfere with the elicitor role of cello-oligosaccharides. It has to be noted that production of turgichelin - together with scabichelin - by *S. scabiei* (BGC#33a) is reported for the first time in this work. Among the other metabolites whose production differed with the metabolomic analysis performed in OBA (28), we could mention bottromycins which were detected in OBA, but with very little production, while we showed that cello-oligosaccharides strongly induce their production. On

the other hand, compounds that were reportedly produced to high levels in OBA – such as concanamycins, thaxtomins and desferrioxamines – were also detected and overproduced upon cello-oligosaccharides addition. Finally, in their metabolomic analysis, Liu and colleagues (28) also highlighted the abundance of CFA-Ile in OBA culture extracts (also shown in (43)). The presence of CFA-Ile in our culture extracts indicates an important role for this molecule in the virulome, even though the addition of cello-oligosaccharides only has a limited positive impact on CFA-Ile production (Figure 1), while we observed massive overexpression via our transcriptomic analysis (Figure 2 and Table 2). Surprisingly, we previously reported in a proteomic study that the abundance of two proteins of the CFA-Ile biosynthetic pathway – SCAB79611 (Cfa2) and SCAB79671 (CFL) – significantly decreased upon cellobiose addition (48). Altogether, these results suggest that the production levels and the expression response of CFA-Ile biosynthetic proteins/genes are highly sensitive to the chosen culture conditions which could explain the important differences between our experimental setup conducted here in minimal media and earlier studies.

Additional metabolites – identified in a previous study (28) – were found in all the tested culture conditions. Production of aerugine, andrachcinidine, Cyclo(L-Val-L-Pro), and a form of the plant hormone auxin (Indole-3-acetic acid - IAA) was more or less influenced by the addition of cello-oligosaccharides, but not dramatically (Figure S2). Only andrachcinidine, an alkaloid metabolite putatively involved in plant defence, was induced by cellobiose and the production of IAA was reduced by a factor two in TDMm + cellobiose and cellotriose. Further research is required to link these metabolites with their currently cryptic BGCs, except for IAA whose biosynthetic genes have previously been identified (49). On the other hand, the presence of additional metabolites described by Liu and colleagues (28) was

581 investigated, but none of them was found in our extracts. These metabolites were: mairine B,
582 bisucaberin, dehydroxynocardamines, and 211 A decahydroquinoline. Informatipeptin – a
583 bioactive compound associated with antimicrobial activity – most-likely produced by
584 BGC#7a could not be detected in any of our extracts.

585 **Cellobiose versus cellotriose as elicitors of virulence**

586 Another question we wanted to address through this work is whether cellotriose could,
587 equally to cellobiose, trigger the "virulome" of *S. scabiei*. Indeed, if most studies have been
588 performed with cellobiose as elicitor - the product being much less expensive and available in
589 larger quantities compared to cellotriose -, earlier works suggest that instead, cellotriose is
590 more likely to emanate from living plants considering the cell wall-related action of
591 thaxtomins. Indeed, cellotriose was shown to be naturally released from actively growing
592 plant tissue, and a treatment with pure thaxtomin A increased the amount of cellotriose
593 exuded by radish seedlings (25). On the other hand, we proposed that cellobiose would rather
594 result from cellulolytic degradation of dead plant material (27). Our metabolomic and
595 transcriptomic analyses revealed that cellobiose and cellotriose are able to induce a similar
596 response. It is however important to note that for most metabolites of the virulome,
597 cellotriose was a stronger inducer compared to cellobiose (Figure 1). Even for germicidins,
598 one of the two metabolites whose production is reduced and not increased by cello-
599 oligosaccharides, cellotriose had a stronger impact. One possible explanation is that, once
600 internalized, cellotriose is hydrolysed to cellobiose and glucose by the beta-glucosidase BglC,
601 therefore further providing the disaccharide eliciting molecule in the intracellular
602 compartment. However, once inside the cell, the hydrolysis of cellobiose by BglC generates

two molecules of glucose that will feed glycolysis (primary metabolism) and no longer act as trigger for the specialized metabolism of *S. scabiei*. In contrast, our transcriptomic analysis suggested that cellobiose was in general a better elicitor compared to cellotriose (Figure 2 and 3). This is not surprising as we showed that the import of cellobiose is faster than that of cellotriose in *S. scabiei* (41), which explains the observed slower transcriptional response. Also, RNA samples were collected after 1 h and 2 h post addition of either cello-oligosaccharides while the extracts for the metabolomic analysis were collected after 96 h of growth. The short-term transcriptional response thus cannot be quantitatively compared to the long-term metabolite production response.

The most important observation is that, for the large majority of BGCs and known metabolites that have been investigated here, we saw a clear correlation between the data obtained via the transcriptomic and metabolomic approaches. Among the few exceptions we can mention the case of the osmoprotectant ectoine, its production being highly induced by both cello-oligosaccharides (Figure 1) while we could not see significant expression changes (Figure 2 and Table 2). The most plausible explanation lies in the fundamental difference in the culture conditions as samples for RNA-seq analyses were collected from liquid cultures just after the addition of the elicitors while metabolite samples were extracted from 96 hours solid cultures. Osmotic protection is expected to be more important after 96-hours cultures at the agar-air interface compared to a couple of hours in liquid cultures with no osmotic changes. The expression of genes involved in ectoine biosynthesis could also be controlled by development-related signals or regulators that are not yet available at RNA sampling time points. Also, no correlation was observed between the strongly reduced germicidin production (Figure 1) and the negligible transcriptional response of the corresponding

626 BGC#29a (Figure 2 and Table 2). Again, the lack of expression change could be explained by
627 the differences in culture conditions. Finally, the transcriptional response of the BGC#20 for
628 bottromycins was too irregular (up-, down-regulation, or no changes according to the elicitors
629 and time points) to make any correlation with the strong overproduction observed via the
630 metabolomic study.

631 **CebR-independent response of most cello-oligosaccharide-dependent BGCs**

632 Surprisingly, except for the thaxtomin gene cluster, only 2 of the 15 other BGCs that showed
633 a strong transcriptional response to cellobiose and cellotriose also showed overexpression in
634 the Δ*cebR* mutant (Figure 4). This result, though unexpected, is in line with the absence of
635 CebR-binding sites in the upstream region of pathway-specific transcriptional activators and
636 core biosynthetic genes of these cello-oligosaccharide expression-dependent BGCs. Through
637 our earlier proteomic analysis, we also observed that many proteins whose production was
638 activated in *S. scabiei* 87-22 by cellobiose did not show production changes in the *cebR* null
639 mutant (48). This could be explained by the possible ability of CebR to bind to "non-
640 canonical" DNA sequences, as previously observed for other transcription factors that also
641 link nutrient sensing and the specialized metabolism (50). Alternatively, cellobiose and
642 cellotriose could be sensed by another and yet unknown transcription factor.

643 **Cryptic metabolites and perspectives**

644 Although strain *S. scabiei* 87-22 is rather well-studied as a model organism, the plurality of
645 its cryptic and/or silent BGCs highlighted a huge reservoir of yet unknown metabolites. Nine
646 of these cryptic BGCs showed a significant response to either both or one of the two cello-

oligosaccharides, suggesting that some of these unknown compounds may also be part of the virulome of *S. scabiei*. The best transcriptional response was observed for BGC#32 (Table 2) involved in the synthesis of a siderophore type metabolite. Together with the transcriptional awakening of BGC#15, the cello-oligosaccharide-dependent response of siderophore-related BGCs further underlines the importance of iron acquisition during host colonization. We also observed the positive expression changes for two BGCs responsible for the production of two bacteriocin type metabolites (BGC#7b and #13). The strain-specificity of these antibacterial peptides is unknown but their synchronized biosynthesis with other host colonization molecules could be seen as a strategy to prevent competing soil-dwelling bacteria to also access the starch reservoir of tubers.

The structure and the bioactivity of the metabolites whose production is triggered by cellobiose and cellotriose is currently under investigation and should lead to the identification of new key virulence determinants associated with the common scab disease.

11. Author statements

11.1 Authors and contributors

Benoit Deflandre: Conceptualization, Formal analysis, Investigation, Methodology, Supervision, Visualization, Writing – original draft

Nudzejma Stulanovic: Formal analysis, Investigation, Software, Visualization, Writing – original draft

Sören Planckaert: Formal analysis, Investigation, Methodology, Writing – review & editing

Sinaeda Anderssen: Data curation, Formal analysis, Methodology, Software, Visualization, Writing – review & editing

Beatrice Bonometti: Investigation

Latifa Karim: Investigation, Methodology, Resources

Wouter Coppieters: Methodology, Project administration, Resources, Supervision

Bart Devreese: Funding acquisition, Methodology, Project administration, Supervision, Writing – review & editing

Sébastien Rigali: Conceptualization, Funding acquisition, Methodology, Project administration, Supervision, Visualization, Writing – original draft

678 ### 11.2 Conflicts of interest

679 The authors declare that there are no conflicts of interest

680 ### 11.3 Funding information

681 The work of S.R. and Be.D was supported by an Aspirant grants from the FNRS (grant
682 1.A618.18) and FRIA grants from the FNRS for S.R. and S.A. (FRIA 1.E.031.18-20) and
683 S.R. and N.S. (FRIA 1.E.116.21). Ba.D. and S.P. were also supported by a Bijzonder
684 Onderzoeksfonds (BOF, grant 01B08915)-basic equipment from the Ghent University special
685 research funds. S.R. is a Fonds de la Recherche Scientifique (FRS-FNRS) senior research
686 associate.

687 ### 11.4 Ethical approval

688 Not applicable

689 ### 11.5 Consent for publication

690 Not applicable

691 ### 11.6 Acknowledgements

692 *[An Acknowledgements section is not compulsory. However, if materials and results were obtained*
693 *from outside the authors' laboratories (e.g. production of antibodies, properties of strains), this must*
694 *be acknowledged.]*

695

696

697 ## 12. References

698 1. Goyer C, Beaulieu C. Host range of streptomycete strains causing common scab. Plant Dis.
699 1997;81(8):901–4.

700 2. Loria R, Bukhalid RA, Fry BA, King RR. Plant pathogenicity in the genus *Streptomyces*. Plant
701 Dis. 1997;81(8):836–46.

702 3. Wanner LA, Kirk WW. *Streptomyces* – from Basic Microbiology to Role as a Plant Pathogen.
703 Am J Potato Res. 2015;92(2):236–42.

704 4. King RR, Lawrence CH, Clark MC. Correlation of phytotoxin production with pathogenicity
705 of *Streptomyces scabies* isolates from scab infected potato tubers. Am Potato J.
706 1991;68(10):675–80.

707 5. Healy FG, Wach M, Krasnoff SB, Gibson DM, Loria R. The *txtAB* genes of the plant pathogen
708 *Streptomyces acidiscabies* encode a peptide synthetase required for phytotoxin thaxtomin A
709 production and pathogenicity. Mol Microbiol. 2000;38(4):794–804.

710 6. King RR, Calhoun LA. The thaxtomin phytotoxins: Sources, synthesis, biosynthesis,
711 biotransformation and biological activity. Phytochemistry [Internet]. 2009;70(7):833–41.
712 Available from: http://dx.doi.org/10.1016/j.phytochem.2009.04.013

713 7. Loria R, Bignell DRD, Moll S, Huguet-Tapia JC, Joshi M V., Johnson EG, et al. Thaxtomin
714 biosynthesis: The path to plant pathogenicity in the genus *Streptomyces*. Antonie Van
715 Leeuwenhoek. 2008;94:3–10.

716 8. Bischoff V, Cookson SJ, Wu S, Scheible W-R. Thaxtomin A affects CESA-complex density,
717 expression of cell wall genes, cell wall composition, and causes ectopic lignification in
718 *Arabidopsis thaliana* seedlings. J Exp Bot. 2009;60(3):955–65.

719 9. Duval I, Beaudoin N. Transcriptional profiling in response to inhibition of cellulose synthesis
720 by thaxtomin A and isoxaben in *Arabidopsis thaliana* suspension cells. Plant Cell Rep.
721 2009;28(5):811–30.

722 10. Tateno M, Brabham C, DeBolt S. Cellulose biosynthesis inhibitors - A multifunctional
723 toolbox. J Exp Bot. 2016;67(2):533–42.

724 11. Li Y, Liu J, Díaz-Cruz G, Cheng Z, Bignell DRD. Virulence mechanisms of plant-pathogenic
725 *Streptomyces* species: An updated review. Microbiology. 2019;165(10):1025–40.

726 12. Khatri BB, Tegg RS, Brown PH, Wilson CR. Temporal association of potato tuber
727 development with susceptibility to common scab and *Streptomyces scabiei*-induced responses
728 in the potato periderm. Plant Pathol. 2011;60(4):776–86.

729 13. Natsume M, Tashiro N, Doi A, Nishi Y, Kawaide H. Effects of concanamycins produced by
730 *Streptomyces scabies* on lesion type of common scab of potato. J Gen Plant Pathol.
731 2017;83:78–82.

732 14. Gimenez-Ibanez S, Chini A, Solano R. How microbes twist jasmonate signaling around their
733 little fingers. Plants. 2016;5 (1)(9):323–9.

15. Fyans JK, Altowairish MS, Li Y, Bignell DRD. Characterization of the coronatine-like phytotoxins produced by the common scab pathogen *Streptomyces scabies*. Mol Plant-Microbe Interact. 2015;28(4):443–54.

16. Bignell DRD, Cheng Z, Bown L. The coronafacoyl phytotoxins: structure, biosynthesis, regulation and biological activities. Antonie Van Leeuwenhoek [Internet]. 2018;111(5):649–66. Available from: https://doi.org/10.1007/s10482-017-1009-1

17. Planckaert S, Deflandre B, de Vries A-M, Ameye M, Martins JC, Audenaert K, et al. Identification of Novel Rotihibin Analogues in *Streptomyces scabies* including Discovery of its Biosynthetic Gene Cluster. Microbiol Spectr. 2021;Accepted(for publication).

18. Argüelles Arias A, Lambert S, Martinet L, Adam D, Tenconi E, Hayette M-P, et al. Growth of desferrioxamine-deficient *Streptomyces* mutants through xenosiderophore piracy of airborne fungal contaminations. FEMS Microbiol Ecol. 2015;91(7):1–9.

19. Kodani S, Bicz J, Song L, Deeth RJ, Ohnishi-Kameyama M, Yoshida M, et al. Structure and biosynthesis of scabichelin, a novel tris-hydroxamate siderophore produced by the plant pathogen *Streptomyces scabies* 87.22. Org Biomol Chem. 2013;11(28):4686–94.

20. Seipke RF, Song L, Bicz J, Laskaris P, Yaxley AM, Challis GL, et al. The plant pathogen *Streptomyces scabies* 87-22 has a functional pyochelin biosynthetic pathway that is regulated by TetR- and AfsR-family proteins. Microbiology [Internet]. 2011 Sep 1 [cited 2017 Aug 4];157(9):2681–93. Available from: http://www.ncbi.nlm.nih.gov/pubmed/21757492

21. Schlösser A, Jantos J, Hackmann K, Schrempf H. Characterization of the binding protein-dependent cellobiose and cellotriose transport system of the cellulose degrader *Streptomyces reticuli*. Appl Environ Microbiol. 1999;65(6):2636–43.

22. Francis IM, Jourdan S, Fanara S, Loria R, Rigali S. The cellobiose sensor CebR is the gatekeeper of *Streptomyces scabies* pathogenicity. MBio. 2015;6(2):1–6.

23. Jourdan S, Francis IM, Kim MJ, Salazar JJC, Planckaert S, Frère J, et al. The CebE/MsiK Transporter is a Doorway to the Cello-oligosaccharide-mediated Induction of *Streptomyces scabies* Pathogenicity. Sci Rep [Internet]. 2016;6:1–12. Available from: http://dx.doi.org/10.1038/srep27144

24. Joshi M V., Bignell DRD, Johnson EG, Sparks JP, Gibson DM, Loria R. The AraC/XylS regulator TxtR modulates thaxtomin biosynthesis and virulence in *Streptomyces scabies*. Mol Microbiol. 2007;66(3):633–42.

25. Johnson EG, Joshi M V., Gibson DM, Loria R. Cello-oligosaccharides released from host plants induce pathogenicity in scab-causing *Streptomyces* species. Physiol Mol Plant Pathol. 2007;71:18–25.

26. Book AJ, Lewin GR, McDonald BR, Takasuka TE, Wendt-Pienkowski E, Doering DT, et al. Evolution of High Cellulolytic Activity in Symbiotic *Streptomyces* through Selection of Expanded Gene Content and Coordinated Gene Expression. PLoS Biol. 2016;14(6):1–21.

27. Jourdan S, Francis IM, Deflandre B, Loria R, Rigali S. Tracking the Subtle Mutations Driving Host Sensing by the Plant Pathogen *Streptomyces scabies*. mSphere. 2017;2(2):1–7.

28. Liu J, Nothias L-F, Dorrestein PC, Tahlan K, Bignell DRD. Genomic and Metabolomic

Analysis of the Potato Common Scab Pathogen *Streptomyces scabiei*. ACS Omega [Internet]. 2021 May 4;6(17):11474–87. Available from: https://pubs.acs.org/doi/10.1021/acsomega.1c00526

29. Bolger AM, Lohse M, Usadel B. Trimmomatic: A flexible trimmer for Illumina sequence data. Bioinformatics. 2014;30(15):2114–20.

30. Langmead B, Salzberg SL. Fast gapped-read alignment with Bowtie 2. Nat Methods. 2012;9(4):357–9.

31. Langmead B, Wilks C, Antonescu V, Charles R. Scaling read aligners to hundreds of threads on general-purpose processors. Bioinformatics. 2019;35(3):421–32.

32. Liao Y, Smyth GK, Shi W. featureCounts: An efficient general purpose program for assigning sequence reads to genomic features. Bioinformatics. 2014;30(7):923–30.

33. Love MI, Huber W, Anders S. Moderated estimation of fold change and dispersion for RNA-seq data with DESeq2. Genome Biol. 2014;15(12):1–21.

34. Blin K, Shaw S, Steinke K, Villebro R, Ziemert N, Lee SY, et al. AntiSMASH 5.0: Updates to the secondary metabolite genome mining pipeline. Nucleic Acids Res. 2019;47(W1):W81–7.

35. Kautsar SA, Blin K, Shaw S, Navarro-Muñoz JC, Terlouw BR, Van Der Hooft JJJ, et al. MIBiG 2.0: A repository for biosynthetic gene clusters of known function. Nucleic Acids Res. 2020;48(D1):D454–8.

36. Vicente CM, Thibessard A, Lorenzi J-N, Benhadj M, Hôtel L, Gacemi-Kirane D, et al. Comparative genomics among closely related *Streptomyces* strains revealed specialized metabolite biosynthetic gene cluster diversity. Antibiotics. 2018;7 (4)(86):1–11.

37. Ōmura S, Shimizu H, Iwai Y, Hinotozawa K, Otoguro K, Hashimoto H, et al. AM-2604 A, a new antiviral antibiotic produced by a strain of *Streptomyces*. J Antibiot (Tokyo). 1982;35(12):1632–7.

38. Dröse S, Altendorf K. Bafilomycins and concanamycins as inhibitors of V-ATPases and P-ATPases. J Exp Biol. 1997;200(Pt1):1–8.

39. Dröse S, Bindseil KU, Bowman EJ, Siebers A, Zeeck A, Altendorf K. Inhibitory Effect of Modified Bafilomycins and Concanamycins on P- and V-Type Adenosinetriphosphatases. Biochemistry. 1993;32(15):3902–6.

40. Hoskisson PA, Seipke RF. Cryptic or silent? The known unknowns, unknown knowns, and unknown unknowns of secondary metabolism. MBio. 2020;11(5):1–5.

41. Jourdan S, Francis IM, Deflandre B, Tenconi E, Riley J, Planckaert S, et al. Contribution of the β-glucosidase BglC to the onset of the pathogenic lifestyle of Streptomyces scabies. Mol Plant Pathol. 2018;19(6):1480–90.

42. Deflandre B, Thiébaut N, Planckaert S, Jourdan S, Anderssen S, Hanikenne M, et al. Deletion of *bglC* triggers a genetic compensation response by awakening the expression of alternative beta-glucosidase. Biochim Biophys Acta - Gene Regul Mech. 2020;1863(10).

43. Bignell DRD, Seipke RF, Huguet-Tapia JC, Chambers AH, Parry RJ, Loria R. *Streptomyces*

scabies 87-22 contains a coronafacic acid-like biosynthetic cluster that contributes to plant-microbe interactions. Mol Plant-Microbe Interact. 2010;23(2):161–75.

44. Lambert S, Traxler MF, Craig M, Maciejewska M, Ongena M, Van Wezel GP, et al. Altered desferrioxamine-mediated iron utilization is a common trait of bald mutants of *Streptomyces coelicolor*. Metallomics. 2014;6(8):1390–9.

45. Yamanaka K, Oikawa H, Ogawa H-O, Hosono K, Shinmachi F, Takano H, et al. Desferrioxamine E produced by *Streptomyces griseus* stimulates growth and development of *Streptomyces tanashiensis*. Microbiology. 2005;151(9):2899–905.

46. Traxler MF, Seyedsayamdost MR, Clardy J, Kolter R. Interspecies modulation of bacterial development through iron competition and siderophore piracy. Mol Microbiol. 2012;86(3):628–44.

47. Craig M, Lambert S, Jourdan S, Tenconi E, Colson S, Maciejewska M, et al. Unsuspected control of siderophore production by N-acetylglucosamine in streptomycetes. Environ Microbiol Rep. 2012;4(5):512–21.

48. Planckaert S, Jourdan S, Francis IM, Deflandre B, Rigali S, Devreese B. Proteomic Response to Thaxtomin Phytotoxin Elicitor Cellobiose and to Deletion of Cellulose Utilization Regulator CebR in *Streptomyces scabies*. J Proteome Res. 2018;17(11):3837–52.

49. Bignell DRD, Huguet-Tapia JC, Joshi M V., Pettis GS, Loria R. What does it take to be a plant pathogen: genomic insights from *Streptomyces* species. In: Antonie van Leeuwenhoek. 2010. p. 179–94.

50. Świątek-Połatyńska MA, Bucca G, Laing E, Gubbens J, Titgemeyer F, Smith CP, et al. Genome-wide analysis of *in vivo* binding of the master regulator DasR in *Streptomyces coelicolor* identifies novel non-canonical targets. PLoS One. 2015;10(4):1–24.

51. Komatsu M, Tsuda M, Omura S, Oikawa H, Ikeda H. Identification and functional analysis of genes controlling biosynthesis of 2-methylisoborneol. Proc Natl Acad Sci U S A. 2008;105(21):7422–7.

52. Seipke RF, Loria R. Hopanoids are not essential for growth of *Streptomyces scabies* 87-22. J Bacteriol. 2009;191(16):5216–23.

53. Jiang J, He X, Cane DE. Biosynthesis of the earthy odorant geosmin by a bifunctional *Streptomyces coelicolor* enzyme. Nat Chem Biol. 2007;3(11):711–5.

54. Bignell DRD, Fyans JK, Cheng Z. Phytotoxins produced by plant pathogenic *Streptomyces* species. J Appl Microbiol. 2014;116(2):223–35.

55. Vior NM, Cea-Torrescassana E, Eyles TH, Chandra G, Truman AW. Regulation of Bottromycin Biosynthesis Involves an Internal Transcriptional Start Site and a Cluster-Situated Modulator. Front Microbiol. 2020;11:1–16.

56. Beauséjour J, Beaulieu C. Characterization of *Streptomyces scabies* mutants deficient in melanin biosynthesis. Can J Microbiol. 2004;50(9):705–9.

57. Bursy J, Kuhlmann AU, Pittelkow M, Hartmann H, Jebbar M, Pierik AJ, et al. Synthesis and uptake of the compatible solutes ectoine and 5-hydroxyectoine by *Streptomyces coelicolor*

A3(2) in response to salt and heat stresses. Appl Environ Microbiol. 2008;74(23):7286–96.

58. Bown L, Li Y, Berrué F, Verhoeven JTP, Dufour SC, Bignell DRD. Coronafacoyl Phytotoxin Biosynthesis and Evolution in the Common Scab Pathogen *Streptomyces scabiei*. Appl Environ Microbiol. 2017;83(19):1–15.

59. Chemler JA, Buchholz TJ, Geders TW, Akey DL, Rath CM, Chlipala GE, et al. Biochemical and Structural Characterization of Germicidin Synthase: Analysis of a Type III Polyketide Synthase that Employs Acyl-ACP as a Starter Unit Donor. J Am Chem Soc. 2012;134(17):7359–7366.

60. Haydock SF, Appleyard AN, Mironenko T, Lester J, Scott N, Leadlay PF. Organization of the biosynthetic gene cluster for the macrolide concanamycin A in *Streptomyces neyagawaensis* ATCC 27449. Microbiology. 2005;151(10):3161–9.

13. Figures and tables

Table 1. **Prediction of BGCs involved in specialized metabolite production in *Streptomyces scabiei* 87-22**

BGC	BGC genes [old locus tag]	BGC length (pb)	Product type	Specialized metabolite	Bioactivity	Most similar BGC (%) Species	Ref / MIBig ID
1a	SCAB_RS00610-00670 [SCAB_1361-1481]	26675	Siderophore	Pyochelin	Iron uptake	Pyochelin (100) *S. scabiei* 87-22	(20)
1b	SCAB_RS00675-00760 [SCAB_1491-1671]	18891	NRPS	Cryptic	Unknown	None	NA
2	SCAB_RS00870-01005 [SCAB_1951-2231]	34118	Betalactone	Cryptic	Unknown	Esmeraldin (4) *S. antibioticus*	BGC0000935
3	SCAB_RS01465-01545 [SCAB_3221-3351]	32892	NRPS	Rothibins	Plant growth inhibitory effect	Rothibins (100) *S. scabiei* RL-34	(17)
4	SCAB_RS01655-01700 [SCAB_3601-3671]	15765	Lanthipeptide	Cryptic	Unknown	None	NA
5	SCAB_RS02290-02370 [SCAB_4951-5131]	19986	Terpene	2-methylisoborneol	Smell of soil	2-methylisoborneol (100) *S. griseus*	(51)
6a	SCAB_RS02505-02545 [SCAB_5421-5511]	11090	Terpene	Isorenieratene	Light harvesting photoprotection	Isorenieratene (100) *S. argillaceus*	BGC0001456
6b	SCAB_RS02550-02590	7346	Terpene	Cryptic	Unknown	Guadinomine (4)	BGC0000998

	[SCAB_5521-5601]					*S.* sp. K01-0509	
7a	SCAB_RS04050-04080 [SCAB_8601-8661]	13988	Lanthipeptide	Informatipeptin	Antimicrobial	Informatipeptin (63) *S. viridochromogenes* DSM 40736	BGC0000518
7b	SCAB_RS04085-04095 [SCAB_8681-8701]	3358	Bacteriocin	Cryptic	Unknown	None	NA
8	SCAB_RS05720-05745 [SCAB_12041-12091]	6531	Butyrolactone	Cryptic	Unknown	Pyocyanine (14) *P. aeruginosa* PA01	BGC0000936
9	SCAB_RS06125-06180 [SCAB_12881-13001]	13913	Terpene	Hopene	Protection against water loss	Hopene (92) *S. coelicolor* A3(2)	(52)
10	SCAB_RS08670-08720 [SCAB_18341-18441]	11906	Siderophore	Cryptic	Unknown	Grincamycin (9) *S. lusitanus*	BGC0000229
11a	SCAB_RS09255-09340 [SCAB_19561-19741]	27673	NRPS-like	Cryptic	Unknown	Stenothricin (11) *S. filamentosus* NRRL 15998	BGC0000431
11b	SCAB_RS09350-09410 [SCAB_19761-19891]	11446	NRPS-like	Cryptic	Unknown	s56-p1 (43) *S.* cp. Soc090715ln-17	BGC0001764
12	SCAB_RS09510 [SCAB_20121]	2207	Terpene	Geosmin	Earthy odorant	Geosmin (100) *S. coelicolor* A3(2)	(53)

13	SCAB_RS09780-09830 [SCAB_20701-20801]	10413	Bacteriocin	Cryptic	Unknown	None	NA
14	SCAB_RS10905-10995 [SCAB_23071-23271]	20828	Terpene	Cryptic	Unknown	FD-594 (7) *S.* sp. Ta-0256	BGC0000222
15	SCAB_RS11635-11660 [SCAB_24651-24711]	9975	Siderophore	Cryptic	Unknown	None	NA
16a	SCAB_RS15070-15100 [SCAB_31761-31841]	18264	NRPS	Thaxtomins	Phytotoxin	Thaxtomin A (100) *S. scabiei* 87-22	(54)
16b	SCAB_RS15145-15225 [SCAB_31961-32131]	19409	Lanthipeptide	Cryptic	Unknown	None	NA
17	SCAB_RS20585-20630 [SCAB_43271-43361]	9782	Type 2 PKS	Spore pigment	Pigment	Spore pigment (75) *S. avermitilis*	BGC0000271
18	SCAB_RS20845-20995 [NA-44151]	42317	NRPS, Type 1 PKS	Cryptic	Unknown	None	NA
19	SCAB_RS22630-22710 [SCAB_47531-47711]	21090	Lanthipeptide	Cryptic	Unknown	None	NA
20	SCAB_RS26995-27050 [SCAB_56591-56711]	17166	Bacteriocin, bottromycin	Bottromycins	Antibacterial	Bottromycin A2 (100) *S. scabiei* 87-22	(55)
21	SCAB_RS27660-27675 [SCAB_57921-57951]	5032	Siderophore	Desferrioxamines	Iron uptake	Desferrioxamines (100) *S.* sp. Id38640	BGC0001478

22	SCAB_RS28265-28270 [SCAB_59231-59241]	1290	Melanin	Melanin	Pigment	Melanin (100) *S. griseus*	(56)
23a	SCAB_RS30025-30125 [SCAB_62881-63081]	30803	Type 1 PKS	Cryptic	Unknown	None	NA
23b	SCAB_RS30085-30160 [NA-63151]	23408	Butyrolactone	Cryptic	Unknown	None	NA
23c	SCAB_RS30120-30205 [NA-63271]	24765	LAP	Cryptic	Unknown	None	NA
23d	SCAB_RS30125-30265 [SCAB_63081-63401]	37334	PKS-like	Cryptic	Unknown	None	NA
24	SCAB_RS33835-33850 [SCAB_70711-70741]	3166	Ectoine	Ectoine	Osmoprotectant	Ectoine (100) *S. scabiei* 87-22	(57)
25	SCAB_RS34860-34975 [SCAB_72851-73081]	24960	NRPS-like	Cryptic	Unknown	None	NA
26	SCAB_RS35245-35325 [SCAB_73651-73801]	17977	Terpene	Cryptic	Unknown	None	NA
27a	SCAB_RS37770-37840 [SCAB_78881-79041]	23685	Type 1 PKS	Cryptic	Unknown	None	NA
27b	SCAB_RS37860-37955 [SCAB_79081-79081]	27749	Indole	Cryptic	Unknown	5-isoprenylindole-3-carboxylate β-D-glycosyl ester (14)	BGC0001483

						S. Sp. RM-5-8	
28	SCAB_RS38095-38165 [SCAB_79581-79721]	31375	Type 1 PKS	Coronafacoyl phytotoxins	Phytotoxin	Coronafacoyl phytotoxin, (100) *S. scabiei* 87-22	(58)
29a	SCAB_RS38310-38370 [SCAB_80021-80131]	15153	Type 3 PKS	Cryptic	Unknown	Daptomycin (11) *S. filamentosus* NRRL 11379	BGC0000336
29b	SCAB_RS38390 [SCAB_80171]	1184	Type 3 PKS	Germicidin	Inhibitor of germination	Germicidin (100) *S. scabiei* 87-22	(59)
30	SCAB_RS39275-39320 [SCAB_82111-NA]	14262	Terpene	Cryptic	Unknown	None	NA
31a	SCAB_RS40100-40220 [SCAB_83841-84101]	94968	Type 1 PKS	Concanamycins	Cytotoxic (antifungal, antineoplastic, anti- protozoal and antiviral)	Concanamycin A (89) *S. neyagawaensis*	(49,60)
31b	SCAB_RS40225-40290 [NA-84261]	13911	Linaridin	Cryptic	Unknown	None	NA
32	SCAB_RS40385-40435 [SCAB_84461-84561]	13579	Siderophore	Cryptic	Unknown	None	NA

33a	SCAB_RS40855-40900 [SCAB_85431-85521]	30019	NRPS	Scabichelin	Iron uptake	Scabichelin (100) *S. scabiei* 87-22	(19)
33b	SCAB_RS40955-41010 [SCAB_85631-85741]	9584	Melanin	Melanin	Pigment	Melanin (57) *S. avermitilis*	BGC0000908
34	SCAB_RS41165-41255 [SCAB_86081-86261]	19524	Terpene	Cryptic	Unknown	None	NA

MICROBIOLOGY SOCIETY

Figure 1. **Relative production of the specialized metabolites of *S. scabiei* 87-22 upon addition of cello-oligosaccharides.** Production levels were assessed in four culture conditions: TDM + maltose 0.5% (TDMm, grey) supplemented with 2.5 mM of cellobiose (+Cellobiose, yellow), cellotriose (+Cellotriose, red) or sucrose (+Sucrose, black). Bar plots display the Area Under the Curve (AUC) of ion peaks normalized to the first replicate of the TDMm condition for each metabolite. Three biological replicates were performed for each culture condition and error bars display the standard deviation observed between three technical replicates.

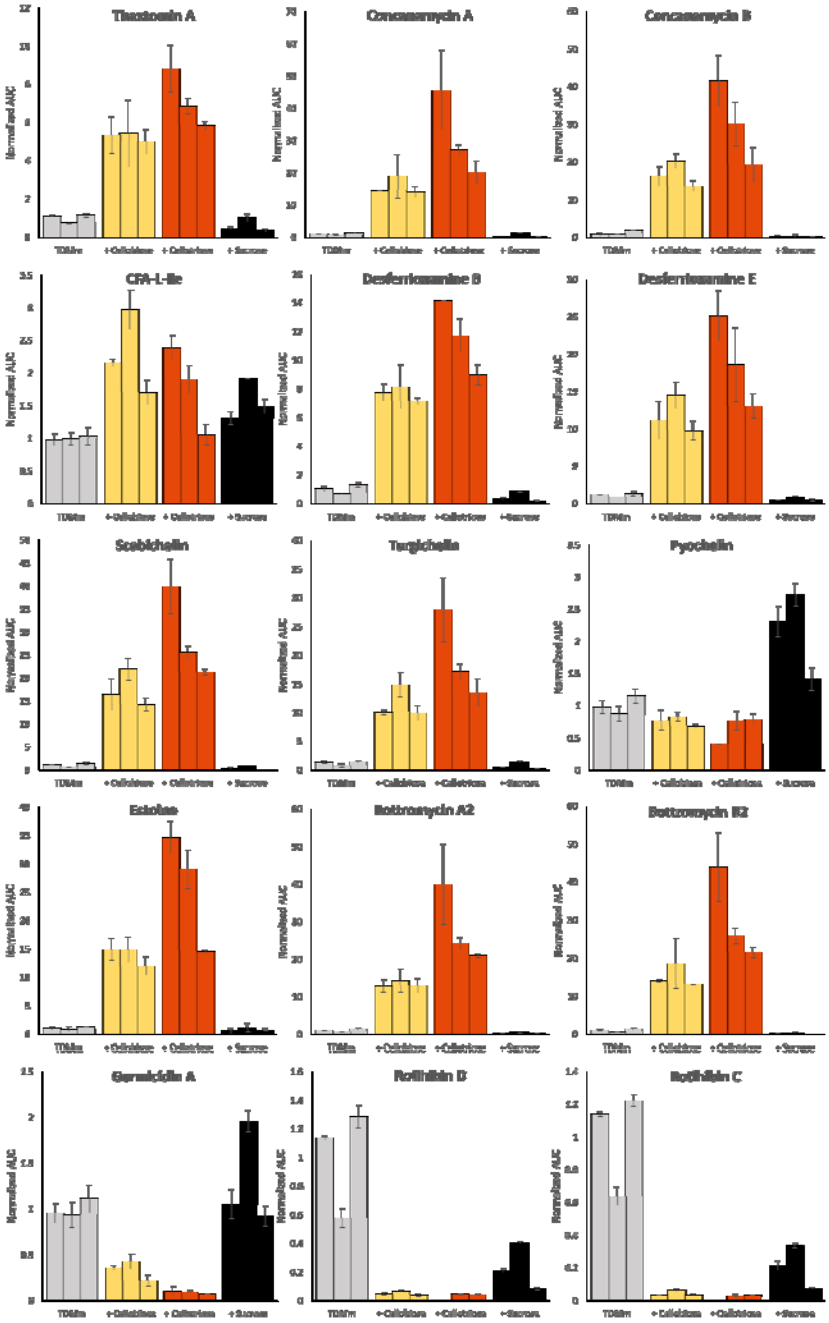

Table 2. Transcriptional response of BGCs (core genes) upon cellobiose and cellotriose supply

BGC	Product	Log2 FC $(Glc)_2$	Log2 FC $(Glc)_3$	BGC	Product	Log2 FC $(Glc)_2$	Log2 FC $(Glc)_3$

1	pyochelin	+ 1.28	+ 0.94	**19**	cryptic	+ 0.33	-
1b	cryptic	+ 2.15	+ 2.39	**20**	bottromycins	- 0.89	-0.15
2	cryptic	-	+ 2.64	**21**	desferrioxamines	+ 3.56	+ 3.63
3	rotihibins	- 0.48	- 0.41	**22**	melanin	-	+ 2.76
4	cryptic	+ 0.47	-	**23a**	cryptic	+ 0.81	-
5	2-methylisoborneol	+ 1.58	+ 1.69	**23b**	cryptic	-	+ 0.85
6a	isorenieratene	- 0.37	+ 0.36	**23c**	cryptic	-	+ 0.85
6b	cryptic	-	-	**23d**	cryptic	-	+ 0.85
7a	informatipeptin	-	-	**24**	ectoine	- 0.30	- 1.39
7b	cryptic	+ 1.08	+ 2.40	**25**	cryptic	+1.19	+ 0.40
8	cryptic	-	-	**26**	cryptic	- 0.53	- 0.59
9	hopene	- 0.81	+ 0.94	**27a**	cryptic	-	-
10	cryptic	- 0.24	- 0.71	**27b**	cryptic	+ 0.86	+ 0.56
11a	cryptic	-	-	**28**	CFA-Ile	+ 3.75	+ 4.25
11b	cryptic	-	-	**29a**	germicidins	-	-
12	geosmin	- 1.09	- 0.85	**29b**	cryptic	-	-
13	cryptic	+ 1.73	+1.71	**30**	cryptic	-	-
14	cryptic	+1.35	+ 0.75	**31a**	concanamycins	+ 1.38	+ 1.44
15	cryptic	+1.51	+1.43	**31b**	cryptic	-	-
16a	thaxtomins	+ 5.16	+ 3.06	**32**	cryptic	+ 3.92	+ 3.21
16b	cryptic	+ 0.55	+ 0.66	**33a**	scabichelin / turgichelin	+ 3.62	+ 3.18
17	WhiE spore pigment	-	-	**33b**	melanin	-	-
18	cryptic	- 0.47	- 0.47	**34**	cryptic	-	-

Figure 2. Expression response of core genes of the known BGCs in presence of cellobiose (A) and cellotriose (B).

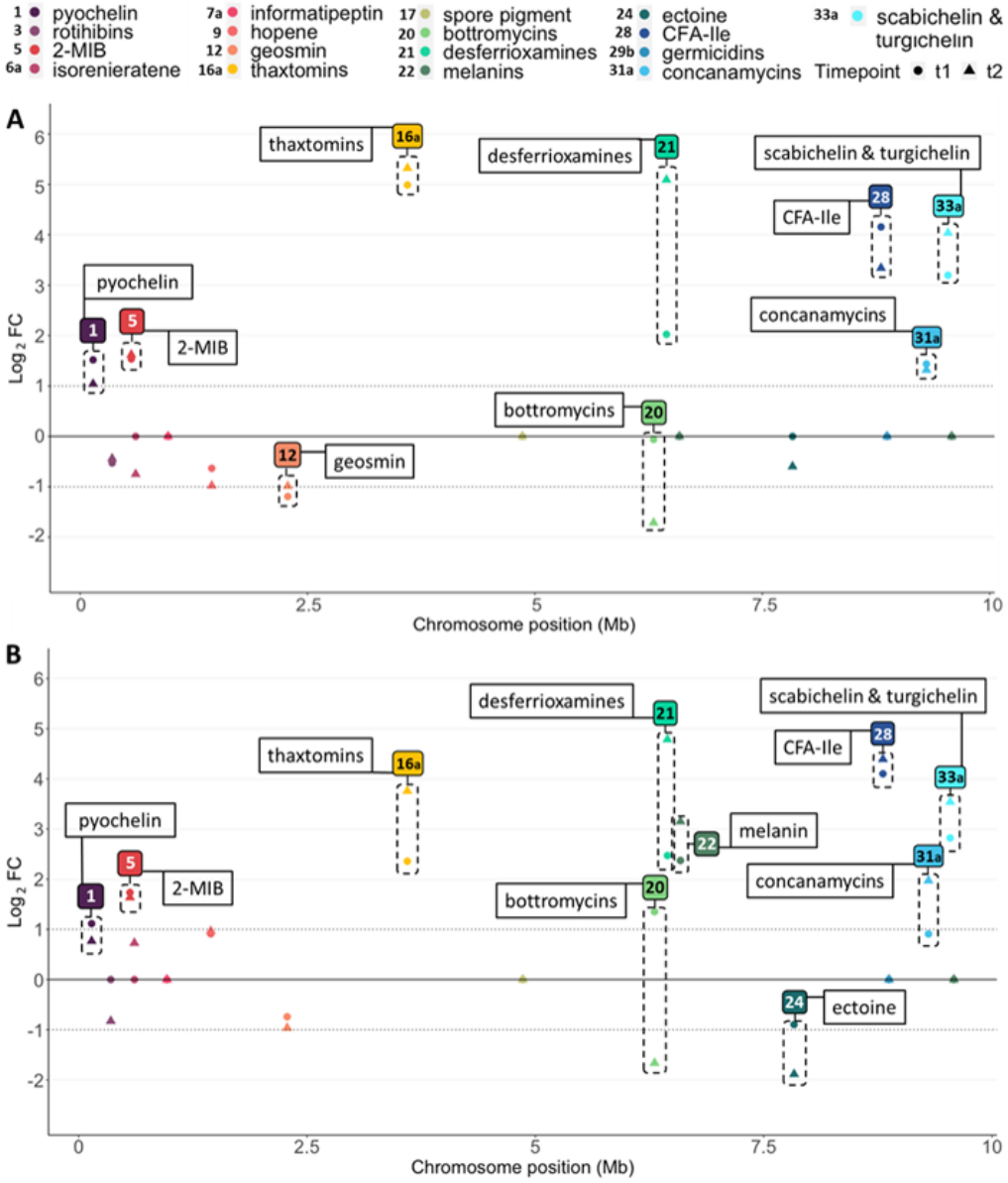

The RNA-seq transcriptomic analysis of *S. scabiei* was conducted in TDM medium (maltose 0.5%) in the presence of cellobiose (A) and cellotriose (B) at time point t1: 1 hour (indicated by circle) and time point t2: 2 hours (indicated by triangle) after induction. The x-axis presents the position of BGCs on the chromosome and the y-axis presents the Log_2 of the expression fold-change (FC) compared to time point 0 (just before cello-oligosaccharide addition). Only data with significant fold-changes (p-value < 0.05) are displayed (BGCs not meeting this criterium have been set to 0). BGCs with a fold-change above or below the threshold -1 > Log_2FC > 1 (at least one time point) are highlighted by a dotted frame.

Figure 3. **Profile of expression level of core genes of the cryptic BGCs in the presence of cellobiose and cellotriose at two time points.**

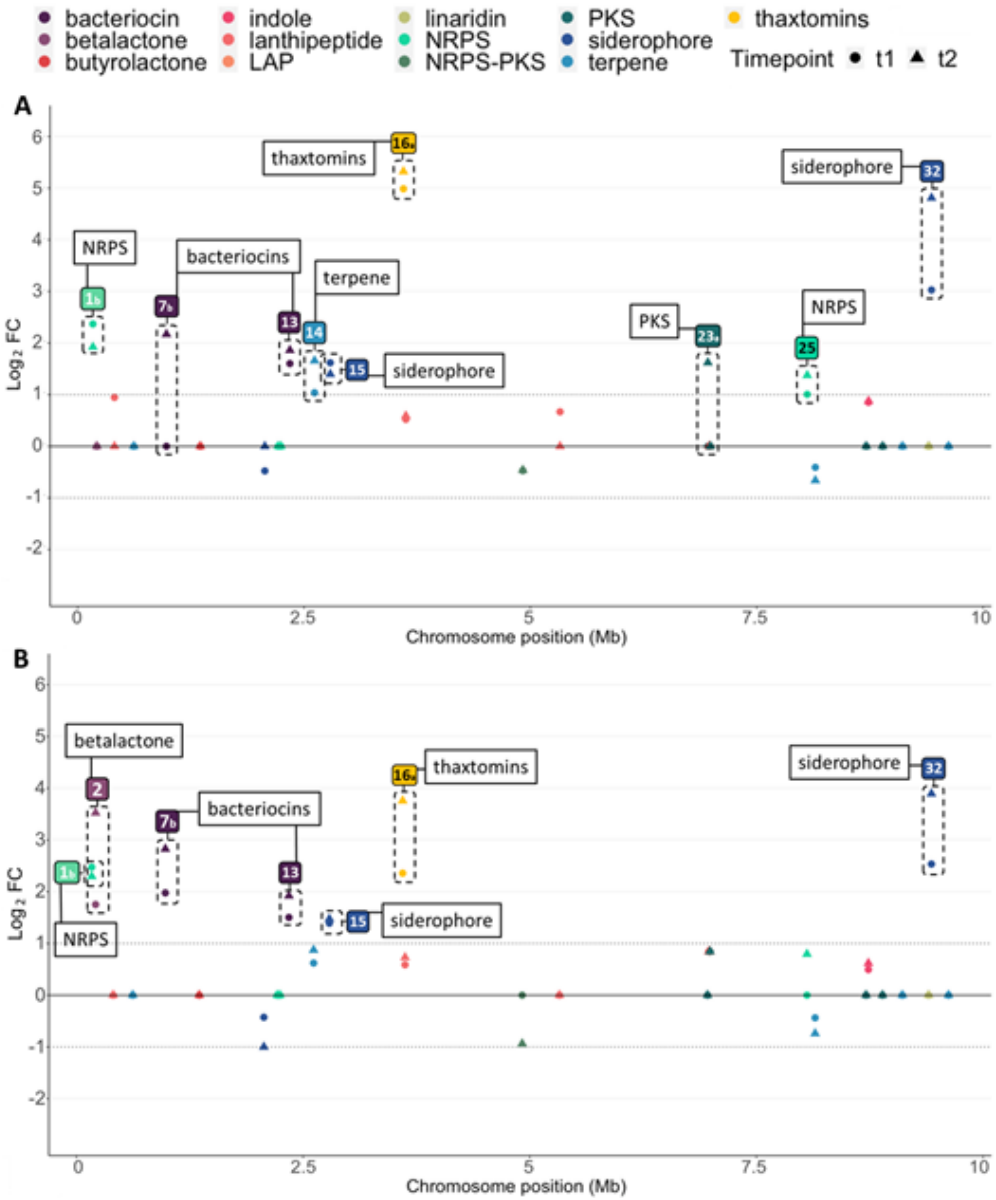

The RNA-seq transcriptomic analysis of *S. scabiei* was conducted in TDM medium (maltose 0.5%) in presence of a) cellobiose and b) cellotriose at time point t1: 1 hour (indicated by circle) and time point t2: 2 hours (indicated by triangle) after induction. The x-axis presents the position of BGCs on the chromosome, whereas the y-axis presents the Log_2 of the expression fold-change (FC) compared to time point 0 (just before cello-oligosaccharide addition). Only data with significant fold-changes (p-value < 0.05) are displayed (BGCs not meeting this criterium have been set to 0). BGCs with a fold-change above or below the threshold -1 > Log_2FC > 1 (at least one time point) are highlighted by a dotted frame.

Figure 4. Volcano plot displaying differentially expressed core BGC genes between the *S. scabiei* wild-type strain and the Δ*cebR* mutant.

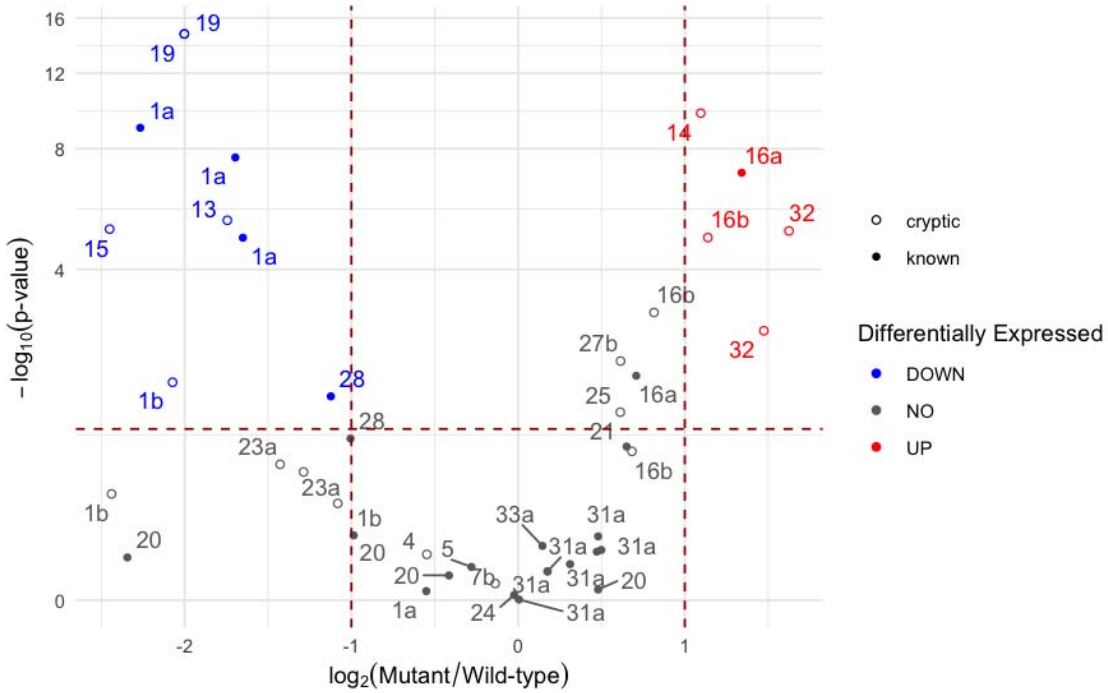

Genes belonging to cryptic BGCs are represented by an empty circle, and those from known BGCs by a full one. Colours indicate the differential expression of each core gene in the Δ*cebR* mutant strain relative to the WT: upregulated (red), downregulated (blue), no significant change (grey). The x-axis displays the Log_2 fold-change (FC) between the mutant and the WT, while the y-axis corresponds to the $-Log_{10}$ (p-value). Significant expression changes were defined as having a p-value < 0.05 and a Log_2FC above or below the given threshold, 1 and -1 respectively ($-1 > Log_2FC > 1$), these limits are represented by dotted red lines on the plot.

Supplementary Figure S1. Detailed expression fold changes (expressed as Log_2) for individual genes of the *txt* cluster (BGC#16a) in cellobiose and cellotriose after 1 or 2 hours of incubation. ND = Not Detected

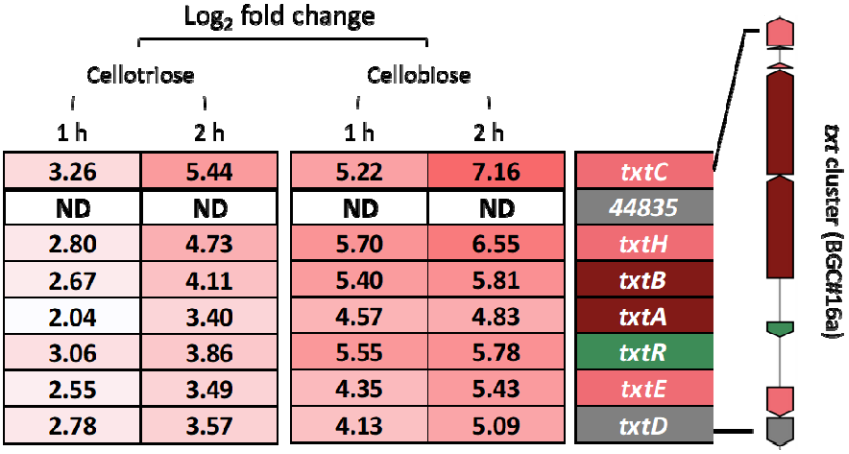

Supplementary Table S1. The MS conditions for the metabolites of interest in MRM mode.

Compound name	*Parent (m/z)*	*Daughter ions (m/z)*	*Dwell (s)*
		Method 1	
Thaxtomin A	439.16	362.11 – 247.11 – 219.11	0.014
Concanamycin A	888.51	679.42 – 515.3 – 502.29 – 396.2 – 378.19 – 348.19 – 196.06	0.014
Concanamycin B	874.49	501.28 – 396.2 – 378.19	0.014
CFA-L-Ile	322.2	191.1 – 163.11 – 145.1 – 119.06	0.117
Desferrioxamine B	561.37	443.32 – 401.29 – 361.32 – 319.3 – 243.19 – 201.17	0.014
Desferrioxamine E	601.36	401.24 – 283.27 – 231.91 – 201.24	0.014
Scabichelin	648.37	518.28 – 346.2 – 259.65	0.014
Turgichelin	621.32	449.23 – 362.2 – 235.06 – 218.11	0.014
Pyochelin	325.06	189.98 – 172 – 145.95 – 127.96	0.117
Bottromycin A2	823.45	637.4 – 494.33 – 476.32 – 363.24 – 315.1	0.014
Bottromycin B2	809.45	623.4 – 480.31 – 462.33 – 349.22 – 315.1	0.014
Bottromycin D2	809.44	623.4 – 494.34 – 476.32 – 363.23 – 301.1	0.014
Bottromycin E2	795.41	609.37 – 466.31 – 448.3 – 349.24 – 315.1	0.014
Germicidin A	197.12	168.08 – 151.07 – 123.12 – 97.03 – 81.07	0.014
Germicidin B	183.1	168.08 – 137.1 – 109.1 – 67.05	0.014
Ectoine	143.08	125.06 – 120.02 – 102.09 – 97.08	0.014
		Method 2	
Rotihibin C	860.62	742.55 – 594.48 – 551.36 – 450.31 – 310.28 – 285.2 – 249.16 – 202.15	0.051
Rotihibin D	874.61	756.55 – 608.48 – 551.36 – 450.31 – 324.28 – 285.2 – 249.16 – 202.15	0.051
IAA	175.7	129.9 – 102.9 – 77.1	0.105
Cyclo(L-Val-L-Pro)	197.13	70.07	0.296
Aerugine	210.06	120.04 – 91.02 – 73.01	0.051
Andrachcinidine	228.2	186.19 – 151.15 – 95.09	0.051

Supplementary Figure S1. Relative production of the specialized metabolites of *S. scabiei* 87-22 upon addition of cello-oligosaccharides.

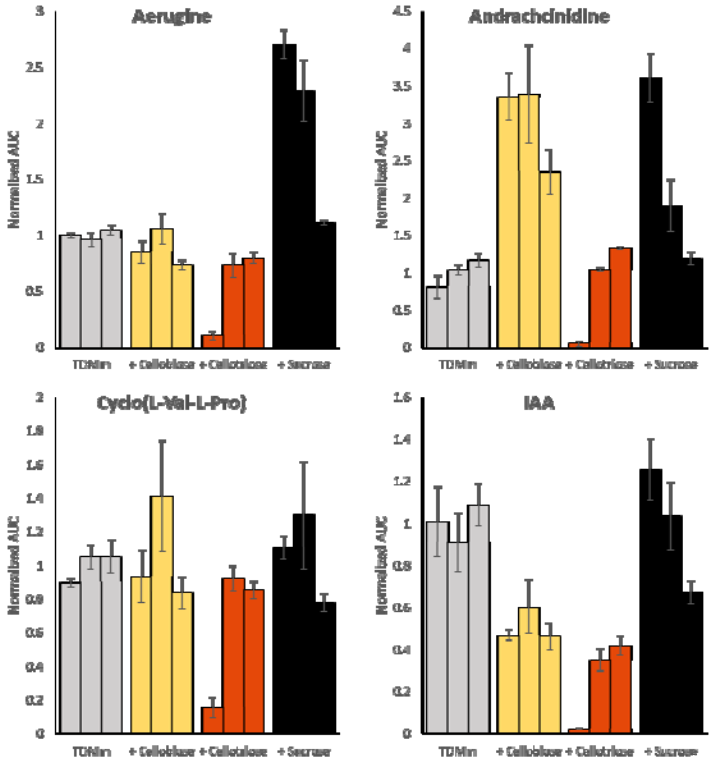

Production levels were assessed in four culture conditions: TDM + maltose 0.5% (TDMm, grey) supplemented with 2.5 mM of cellobiose (+Cellobiose, yellow), cellotriose (+Cellotriose, red) or sucrose (+Sucrose, black). Bar plots display the Area Under the Curve (AUC) of ion peaks normalized to the first replicate of the TDMm condition for each metabolite. Three biological replicates were performed for each culture condition and error bars display the standard deviation observed between three technical replicates.

Supplementary Table S2. List of the core biosynthetic gene(s) and their predicted function for each BGC

BGC	Old locus tag	Locus tag	Gene function	Specialized metabolite
1a	SCAB_2411	SCAB_RS30635	AMP-binding protein	Pyochelin
	SCAB_2471	SCAB_RS30985	Amino acid adenylation domain-containing protein	
	SCAB_2481	SCAB_RS30970	Non-ribosomal peptide synthetase	
1b	SCAB_2541	SCAB_RS30665	Fatty acyl-AMP ligase	Cryptic
	SCAB_2551	SCAB_RS30650	Fatty acyl-AMP ligase	
	SCAB_2571	SCAB_RS30640	AMP-binding protein	
2	SCAB_2011	SCAB_RS30900	AMP-binding protein	Lysine
	SCAB_2061	SCAB_RS30715	Acyl-CoA ligase	
	SCAB_2071	SCAB_RS30710	6-hydroxy-3-ketooctanoate aldolase	
	SCAB_2131	SCAB_RS30620	long-chain fatty acid--CoA ligase	
3	SCAB_3221	SCAB_RS31405	Non-ribosomal peptide synthetase	Rothilins
	SCAB_3261	SCAB_RS31485	Fatty acyl-AMP ligase	
	NA	SCAB_RS31525	Non-ribosomal peptide synthetase	
4	SCAB_3821	SCAB_RS31675	Phosphotransferase	Cryptic
5	SCAB_3041	SCAB_RS32330	Terpene synthase family protein	2-methylisoborneol
6a	SCAB_3441	SCAB_RS32515	Phytoene/squalene synthase family protein	Isoprenoid
	SCAB_3481	SCAB_RS32535	NAD(P)-binding protein	
7a	SCAB_3811	SCAB_RS34035	Protein kinase/lanthionine synthetase C family protein	Informaticaspin
7b	SCAB_3851	SCAB_RS34085	hypothetical protein	Cryptic
8	SCAB_12361	SCAB_RS33740	AfsA/SCAB-like protein	Cryptic
9	SCAB_12791	SCAB_RS34140	Squalene--hopene cyclase	Hopene
	SCAB_12891	SCAB_RS34175	Presqualene diphosphate synthase HpnD	
	SCAB_12901	SCAB_RS34180	Squalene synthase HpnC	
10	SCAB_18891	SCAB_RS36695	Iron transporter	Cryptic
	SCAB_18901	SCAB_RS36700	IucA/IucC family siderophore biosynthesis protein	
11a	SCAB_19891	SCAB_RS39515	Non-ribosomal peptide synthetase	Cryptic
12	SCAB_20111	SCAB_RS39510	terpene synthase family protein	Geosmin
13	SCAB_20791	SCAB_RS39810	DUF692 domain-containing protein	Cryptic
14	SCAB_23181	SCAB_RS16980	3l trans,poly cis decaprenyldiphosphate synthase	Cryptic
15	SCAB_24881	SCAB_RS11890	Iron transporter	Cryptic
16a	SCAB_47291	SCAB_RS14280	Amino acid adenylation domain-containing protein	Thaxtomin A
	SCAB_47301	SCAB_RS14285	Amino acid adenylation domain-containing protein	
16b	SCAB_47281	SCAB_RS14270	Lanthionine cyclodehydratase	Cryptic
	SCAB_47291	SCAB_RS14280	Lanthionine synthetase C family protein	
	SCAB_32031	SCAB_RS15185	hypothetical protein	
17	SCAB_43301	SCAB_RS36000	Beta-ketoacyl-[acyl-carrier-protein] synthase family protein	Spore pigment
	SCAB_43311	SCAB_RS36005	Polyketide beta-ketoacyl synthase	
18	SCAB_43961	SCAB_RS36905	hybrid non-ribosomal peptide synthetase/type I polyketide synthase	Cryptic
19	SCAB_44641	SCAB_RS37275	Protein kinase/lanthionine synthetase C family protein	Lysine
20	SCAB_44661	SCAB_RS37290	RiPP maturation radical SAM protein 1	Betaenone
	SCAB_44671	SCAB_RS37295	Alpha/beta hydrolase	
	SCAB_50021	SCAB_RS37625	RiPP maturation radical SAM protein 1	
	SCAB_50091	SCAB_RS37680	RiPP maturation radical SAM protein 1	
21	SCAB_57911	SCAB_RS37680	IucA/IucC family siderophore biosynthesis protein	Desferrioxamines
22	SCAB_59251	SCAB_RS38285	Tyrosinase co-factor	Melanin
23a	SCAB_62841	SCAB_RS39035	Acyltransferase domain-containing protein	Cryptic
23b	SCAB_63511	SCAB_RS39100	hypothetical protein	Cryptic
	SCAB_63521	SCAB_RS39105	hypothetical protein	
	SCAB_63111	SCAB_RS39140	Secondary metabolite regulator	
	NA	SCAB_RS39135	SagB/ThcOx family oxidoreductase	
	SCAB_63131	SCAB_RS39180	TOMM precursor leader peptide-binding protein	
23c	SCAB_63111	SCAB_RS39140	Secondary metabolite regulator	Cryptic
	NA	SCAB_RS39135	SagB/ThcOx family oxidoreductase	
	SCAB_63131	SCAB_RS39180	TOMM precursor leader peptide-binding protein	
	SCAB_63141	SCAB_RS39185	Secondary metabolite synthase protein	
23d	SCAB_63111	SCAB_RS39140	Secondary metabolite regulator	Cryptic
	NA	SCAB_RS39135	SagB/ThcOx family oxidoreductase	
	SCAB_63131	SCAB_RS39180	TOMM precursor leader peptide-binding protein	
	SCAB_63251	SCAB_RS39195	Secondary metabolite synthase protein	
	SCAB_63261	SCAB_RS39210	Secondary metabolite biosynthesis protein	
24	SCAB_70731	SCAB_RS35840	Ectoine synthase	Ectoine
25	SCAB_72891	SCAB_RS34930	Formate dehydrogenase	Cryptic
26	SCAB_73741	SCAB_RS35280	hypothetical protein	Cryptic
27a	SCAB_78961	SCAB_RS37605	Acyltransferase domain-containing protein	Cryptic
27b	SCAB_79031	SCAB_RS37640	Tryptophanase	Lysine
28	SCAB_79031	SCAB_RS38130	Type I polyketide synthase	Coronafacoyl phytotoxins
	SCAB_79061	SCAB_RS38135	Type I polyketide synthase	
29b	SCAB_80171	SCAB_RS38380	Polyketide synthase	Germicidins
30	SCAB_82161	SCAB_RS39305	Cyclase	Cryptic
31a	SCAB_83871	SCAB_RS40110	Type I polyketide synthase	Lanosamycin
	SCAB_83891	SCAB_RS40115	Type I polyketide synthase	
	SCAB_83901	SCAB_RS40120	Type I polyketide synthase	
	SCAB_83911	SCAB_RS40125	Type I polyketide synthase	
	SCAB_83921	SCAB_RS40130	Type I polyketide synthase	
	SCAB_83931	SCAB_RS40135	Type I polyketide synthase	
31b	SCAB_84161	SCAB_RS40250	hypothetical protein	Cryptic
32	SCAB_84411	SCAB_RS40405	Heterocyst biosynthesis protein	Cryptic
	SCAB_84421	SCAB_RS40410	Iron transporter	
33a	SCAB_84671	SCAB_RS40575	Non-ribosomal peptide synthetase	Arabirubin / Ikarugamycin
33b	SCAB_85091	SCAB_RS40985	Tyrosinase	Melanin
34	NA	SCAB_RS41210	Squalene/phytoene synthase family protein	Cryptic